Published in Dalton Transactions, 2020, 49, 8143-8161

Heterobimetallic μ_2-carbido Complexes of Platinum and Tungsten

Liam K. Burt[a] and Anthony F. Hill[a,*]

The tungsten-platinum μ-carbido complex [WPt(μ-C)Br(CO)$_2$(PPh$_3$)$_2$(Tp*)] (Tp* = hydrotris(dimethylpyrazol-1-yl)borate) undergoes facile substitution of both bromide and phosphine ligands to afford a diverse library of μ-carbido complexes that includes [WPt(μ-C)Br(CO)$_2$(dppe)(Tp*)], [WPt(μ-C)(NCMe)(CO)$_2$(PPh$_3$)$_2$(Tp*)]OTf, [WPt(μ-C)(S$_2$CNEt$_2$)(CO)$_2$(PPh$_3$)(Tp*)], [WPt(μ-C)(bipy)(CO)$_2$(PPh$_3$)(Tp*)]PF$_6$, [WPt(μ-C)(phen)(CO)$_2$(PPh$_3$)(Tp*)]PF$_6$, [WPt(μ-C)(terpy)(CO)$_2$(Tp*)]PF$_6$, [WPt(μ-C)(CO)$_2$(PPh$_3$)(Bp*)(Tp*)], [WPt(μ-C)(CO)$_2$(PPh$_3$)(Tp*)$_2$] and [WPt(μ-C)(bipy)(CO)$_2$(PPh$_3$)(Bm)(Tp*)], most of which have been structurally charcaterised.

Introduction

Bimetallic complexes containing a μ-carbido ligand have grown in number in recent years such that sufficient examples exist to allow their categorisation into four distinct groups (Chart 1) that vary in the electronic localisation along the linear[1-3] or more recently bent[4] MCM spines. Classes **A**[1] and **C**[3] provide the same number of valence electrons to each metal, whilst Class **B**[2] involves distinct triple and single metal-carbon bonds, providing three and one valence electrons, respectively, to the metals. Although Class C is represented as having a triple bond to one metal to reflect the σ and two π-components, the covalent bonding is best classified as 'X_2' to one metal and 'L' to the other.

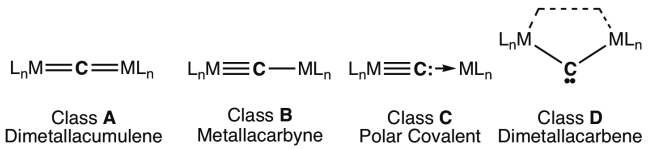

Chart 1. Distinct μ-Carbido Bonding Modes.[1-4]

Given the disparate electronic needs of the two metals, it is not surprising that with the exception of one example, [Ru$_2$(μ-C)(μ:σ,η^6-IMesH$_2$)Cl$_3$(IMesH$_2$)] (IMesH$_2$ = *N,N'*-dimesitylimidazolylidin-2-ylidene),[2c] all others are heterobimetallic in nature. Synthetic routes to Class **B** μ-carbido complexes (Chart 2) include (i) scission of a ruthenium propynyl ligand by [W$_2$(O^{t}Bu)$_6$];[2a] (ii) nucleophilic substitution at a chlorocarbyne ligand by [Fe(CO)$_2$(η-C$_5$H$_5$)]$^-$;[2b] (iii) bimolecular degradation of a methylidene ligand;[2c] (iv) nucleophilic metal-halide metathesis by lithiocarbynes [M(≡CLi)(CO)$_2$(Tp*)] (M = Mo, W; Tp* = hydrotris(dimethylpyrazol-1-yl)borate);[2d-g] (v) rearrangement of a Class **A** dimetallacumulene;[2i] (vi) insertion of a metal into the C–Se bond of a selenocarbonyl ligand[2f,2m] and (vii) oxidative addition of bromocarbynes to zerovalent group 10 metal centres.[2j,k] This last approach has recently provided expedient access to the tungsten-platinum μ-carbido complex [WPt(μ-C)Br(CO)$_2$(PPh$_3$)$_2$(Tp*)] (**1**)[2k] which is thermally stable. This is in contrast to the analogous complexes [WNi(μ-C)Cl(CO)$_2$(PEt$_3$)$_2$(Tp*)] (**2**)[2d] and [WPd(μ-C)Br(CO)$_2$(PPh$_3$)$_2$(Tp*)] (**3**)[2j] which convert spontaneously and irreversibly to μ-phosphoniocarbyne derivatives [WM(μ-CPR$_3$)Br(CO)$_2$(PR$_3$)$_n$(Tp*)] (M = Ni, R = Et, n = 1; M = Pd, R = Ph, n = 0, 1). Given the comparative scarcity of Class **B** carbido complexes, complex **1** therefore appeared to provide a potentially versatile platform for developing platinum carbido chemistry by virtue of the characteristic propensity of *d*^{8}-square planar complexes to enter into ligand substitution reactions. We report herein an exploration of this synthetic potential, which has led to the identification of an extensive library of new Class **B** carbido complexes.

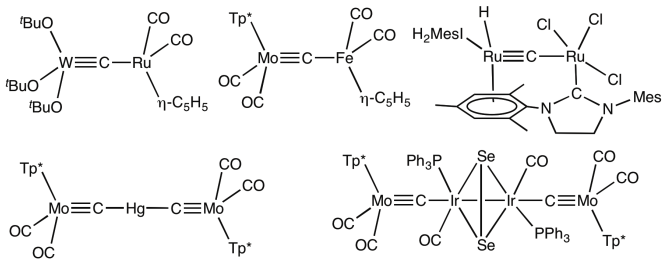

Chart 2. Representative Class **B** μ-carbido complexes.[2]

Results and Discussion

The complex **1**, described in a recent preliminary communication,[2j] arises from the reaction of [W(≡CBr)(CO)$_2$(Tp*)][5] with [Pt(PPh$_3$)$_4$] in refluxing toluene, conditions that attest to its thermal stability. The complex is replete with functionalities that present informative spectroscopic signatures (IR: ν_{CO}; NMR: ^{1}H, ^{13}C, ^{11}B, ^{31}P, ^{183}W and ^{195}Pt nuclei), consideration of which not only confirms the *trans* geometry at platinum but also indicates that the molecule adopts two different isomers with respect to rotation about the WCPt spine. Although this isomerism does not impact on the chemistry to be described, it does reflect the considerable steric bulk presented by the Tp* ligand which is accommodated by inter-digitation of ligands on the adjacent platinum centre. It is useful here to consider the features of **1** (Figure 1) in more detail so as to provide a benchmark for the new derivatives that follow.

[a] *Research School of Chemistry, The Australian National University, Canberra, ACT 0200, Australia. Email: a.hill@anu.edu.au*

CCDC 1997712-1997719 contain the supplementary crystallographic data for this paper and are available free of charge from The Cambridge Crystallographic Data Centre.

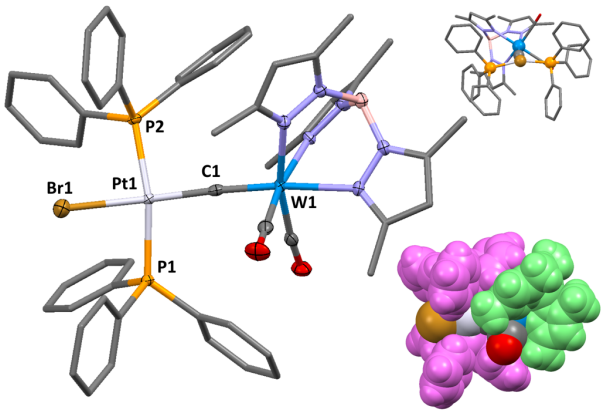

Figure 1. Molecular structure of **1** in a crystal (50% displacement ellipsoids, pyrazolyl and phenyl groups simplified, hydrogen atoms omitted). Selected bond lengths (Å) and angles (°): Pt1–Br1 2.5274(7), Pt1–P1 2.3265(12), Pt1–P2 2.3256(12), Pt1–C1 1.934(6), W1–C1 1.856(6), W1–C1–Pt1 169.2(3), C1–Pt1–Br1 169.19(15), P2–Pt1–P1 160.28(5). Insets = view along Br1…Pt1 vector and space filling representation indicating steric clash between Tp* (green) and phosphine (cerise) ligands.

There are sufficiently few known examples of structurally characterised Class **B** carbido complexes that salient data may be summarised for future reference (Table 1) and these support their description as involving triple and single bonds to the respective metals. Even from this small number of examples, it is apparent that quite significant bending of the M≡C–M' spine is tolerated (160.3-180°) in response to inter-ligand or intermolecular packing interactions. Deformations in the geometry at platinum from ideal square planar are evident, with the phosphines bent away from the sterically imposing '(Tp*)$(CO)_2$WC' fragment in **1** towards the bromide ligand (P2–Pt1–P1 160.28(5)°). The bromide, however, has weak associations with methyl groups on the adjacent molecule (C-H···Br: 2.73, 2.87 Å), clouding immediate inferences about the *trans*-influence of the carbido ligand, that are, however, established for examples to follow. To circumvent this, the gas-phase molecular structure of the simplified analogue [WPt(μ-C)Br$(CO)_2(PMe_3)_2$(Tp)] (**1Br***; Tp = hydrotris(pyrazolyl)borate) was interrogated at the DFT:ωB97X-D/6-31G*/LANL2Dζ level of theory (See ESI, Table 1, hereafter calculated structures are designated by an asterisk). With the smaller PMe_3 ligand replacing bulky PPh_3, and excision of the Tp* methyl substituents, the P–Pt–P angle more closely approaches (174.0°) but still does not reach the ideal of 180° as one phosphine methyl group still nestles between proximal pyrazolyl groups. There is, however, a contraction of both the W≡C 1.827 Å) and C–Pt (1.921 Å) bond lengths within the more compact molecule and the W≡C–Pt spine is slightly more linear (167.8°). The Lowdin bond orders were determined to be 2.275 and 1.247 for W≡C and C–Pt, respectively while Pt–Br (1.004) and Pt–P (0.973, 0.962) bond orders are close to unity. Whilst metal-carbido infrared absorptions have been rarely identified for class **A** carbido complexes[1d,k,l] they have yet to be observed for class **B** examples, which is perhaps counter-intuitive in that the asymmetry of the M≡C–M' spine should in principle result in more intense absorptions. The frequency calculation performed for **1Br*** reveals vibrations primarily associated with the W≡C–Pt stretching modes at 1024 (w) 1031 (m) cm^{-1}. The latter is reasonably intense (0.61 *vs* ν_2(CO) = 1.00) and appears to slightly higher frequency of those observed for class **A** (M=C=M) examples [$Re_2(\mu\text{-}C)(CO)_4(\eta\text{-}C_5H_5)_2$] (1019 cm^{-1})[1d] and [WRe(μ-C)$(CO)_3$(NO)(η-C_5H_5)(Tp*)] (968 cm^{-1}).[1l]

Table 1. Selected structural and spectroscopic data for known Class **B** carbido complexes $L_nM{\equiv}C{-}ML_n$[2]

L_nM	$M'L_n$	M≡C [Å]	C–M' [Å]	M≡C–M' [°]	δ_C ppm
(^{t}BuO)$_3$W	Ru$(CO)_2$(Cp)	1.75(2)	2.09(2)	177(2)	237.3
(Tp*)$(CO)_2$Mo	Fe$(CO)_2$(Cp)	1.819(6)	1.911(8)	172.2(5)	381
Cl_3(IMesH$_2$)Ru	RuH(IMesH$_2$)$_2$	1.698(4)	1.895(4)	160.3(2)	414.0
$Cl_3(PCy_3)$Ru	PtCl(py)$_2$	1.669(1)	1.900(1)	166.2(1)	354.6
(μ-dppm)Cl_3Ru[a]	PtCl(μ-dppm)	1.698(2)	1.852(2)	177.0(2)	361.9
		1.692(4)	1.853(4)	180	
(μ-dcpm)Cl_3Ru	PtCl(μ-dcpm)	1.694(2)	1.842(2)	166.2(1)	362.0
(dcpm)$Cl_3(H_2O)$Ru	PtCl(PCy_3)	1.694(5)	1.890(5)	170.5(3)	360.0
(PCy_3)$(OH_2)Cl_3$Ru	PtCl(Hpz)$_2$	1.692(3)	1.899(3)	164.3(2)	358.5
(HNPAd)ClRu^{2+}	PtCl(py)$_2$	1.687(4)	1.923(4)	176.5(2)	353.6
(Tp*)$(CO)_2$W	NiCl(PEt_3)$_2$ (**2**)	1.867(4)	1.808(4)	174.8(2)	484.0
(Tp*)$(CO)_2$Mo	PtBr(PPh_3)$_2$	1.828(3)	1.951(3)	174.0(2)	339.0
(Tp*)$(CO)_2$W	PtBr(PPh_3)$_2$ (**1**)[2j]	1.856(6)	1.934(6)	169.2(3)	318.6
(Tp*)$(CO)_2$Mo	PdBr(PPh_3))$_2$[b]	1.807(6)	1.923(6)	166.3(3)	330.8
(Tp*)$(CO)_2$Mo	PdBr(dppe)[c]	1.79(1)	2.01(1)	167.9(8)	375.9
(Tp*)$(CO)_2$Mo	Ir(CO)(PPh_3)(Se}$_2$	1.843(5)[a]	1.973(5)	169.8(3)	286.1
(Tp*)$(CO)_2$W	Pt(terpy)$^+$ [**8**]$^+$	1.835(5)	1.938(5)	176.3(3)	367.7
(Tp*)$(CO)_2$W	PtCl(phen-CW)	1.853(14)	1.890(14)	173.4(9)	331.3
(Tp)$(CO)_2$W[d]	PtBr(PMe_3)$_2$ (**1Br***)	1.827	1.921	167.8	
(Tp)$(CO)_2$W[e]	PtCl(PMe_3)$_2$ (**1Cl***)	1.850	1.920	177.0	

[a]Two crystal polymorphs. [b]Mean values. [c]Imprecise structural model (R_1 = 0.096) due to limited data quality. [d]DFT:ωB97X-D/6-31G*/LANL2Dζ; [illegible] = 2.602 Å; ν_{CO} = 1956, 1866 cm^{-1}; ν_{WCPt} = 1024, 1031 cm^{-1}. [e]DFT:B3LYP/6-31G*/LANL2Dζ[illegible] = 2.517 Å; ν_{CO} = 1929, 1857 cm^{-1}; ν_{WCPt} = 1017, 1027 cm^{-1}. Abbreviations: dcpm = bis(dicyclohexylphosphino)methane, dppm = bis(diphenylphosphino)methane, NPAd = bis(diadamantylphosphinoethyl)amido, terpy = 2,2':6',2''-terpyridyl.

Lin and Marder have provided a benchmark computational study on the *trans* influence of a range of ligands 'X' in the complexes *trans*-[Pt(X)Cl$(PMe_3)_2$][6] and whilst that study focused on quantifying the superlative *trans*-influence of σ-boryl ligands, it included the parent hydrocarbyls X = C_2H_5, $CH{=}CH_2$ and C≡CH. The isolobal analogy between alkynes and carbynes[7] has long guided the exploration and post-rationalisation of much carbyne chemistry, not least in the extensive work of Stone on the strategic construction of polymetallic assemblies.[8] Accordingly, some analogy between Class **B** carbido complexes and σ-alkynyls might be entertained. To allow direct comparison, we have also explored the hypothetical complex [WPt(μ-C)Cl$(CO)_2(PMe_3)_2$(Tp)] (**1Cl***) at the same level of theory used in the Lin-Marder study (DFT:B3LYP/6-31G*/LANL2Dζ, Figure 2; ν_{WCPt} = 1027 cm^{-1}, LBO: W≡C 2.213, Pt–C 1.299) and whilst the geometric features of the W≡C–Pt spine are generally comparable to those for **1Br***, the resulting Pt–Cl bond length (2.517 Å) is somewhat longer than found for the ethynyl model (Table 2), falling between those for vinyl and alkyl ligands.

Table 2. Calculated geometric parameters[a] for the complexes *trans*-[Pt(R)Cl(PMe_3)$_2$] (from ref. 6)

R	C–Pt [Å]	Pt–Cl [Å]
CH_2CH_3[b]	2.093	2.531
$CH{=}CH_2$[b]	2.019	2.510
C_6H_5[b]	2.035	2.496
C≡CH[b]	1.968	2.448
C≡W(CO)$_2$(Tp)[c] (**1Cl***)	1.920	2.517

[a]DFT:B3LYP/6-31G*/LANL2Dζ. [b]Taken from reference 6. [c]P-Pt-P = 170.6°.

We may therefore conclude that the *trans*-influence exerted by the X = (Tp)(CO)$_2$W≡C unit is greater than that of an alkynyl ligand, however, that said, caveats need to be noted: (i) There is clearly a steric impact on the platinum geometry for **1Cl*** that is essentially absent for the cylindrical X = C≡CH case; (ii) Amongst σ-organyls, σ-alkynyls show rather weak *trans* influences, a phenomenon that Lin and Marder, in developing concepts proposed by Muir and Muir,[9] interpret in terms of rather modest π-retrodonation helping to reduce the destabilising effect of occupied d^8-platinum and chloride orbitals of Pt–Cl π-symmetry. (iii) Current synthetic methodologies limit significant variations on the carbyne end of the Class **B** metallacarbyne. As these constraints are overcome, we may anticipate a far broader spectrum of π-basicity with respect to the carbyne metal and co-ligands. Towards the Schrock end of the Fischer-Schrock carbyne continuum, we may anticipate carbido ligands with energetically elevated and occupied M≡C π-orbitals and accordingly, enhanced *trans* influence. In passing, we also note that the three pyrazolyl groups provide an internal reference for comparing carbido and carbonyl ligands. The W–N bond length *trans* to the carbido is significantly longer (2.361 Å) than the average of the two remaining W–N bond lengths (2.261 Å) despite this being remote from any inter-ligand steric congestion.

Continuing with the alkynyl analogy, we note that despite the vastly different steric profiles of the carbido fragment and the slender ethynyl ligand, of the series the carbido complex has by far the shortest Pt–C bond length (1.920 Å). This perhaps argues for a considerable degree of Pt-C π-overlap, and this is indicated by the topology of the HOMO-6 (Figure 2). This orbital is π-bonding from tungsten, through carbon to platinum but π-anti-bonding between Pt and Cl. It is noteworthy that in the absence of this Pt–C dπ-pπ interaction, the corresponding Pt–Cl π-anti-bonding orbital in [Pt(C_2H_5)Cl(PMe_3)$_2$] represents the HOMO. The experimentally determined Pt–C bond length for **1** (1.934(6) Å) is again significantly shorter (1.943(6) Å) than that found experimentally for [Pt(C≡CCMe_2O_2H)Br(PPh_3)$_2$] (1.990(1) Å)[10] despite the disparity in steric profiles.

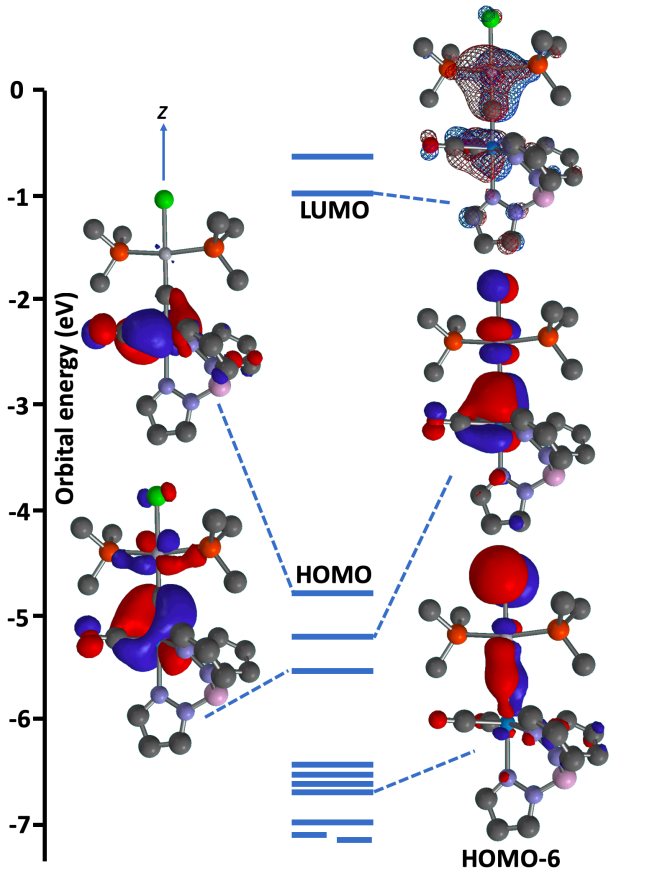

Figure 2. Optimised geometry (DFT:B3LYP/6-31G*/LanL2Dζ) and frontier orbitals of interest for the hypothetical complex [WPt(μ-C)Cl(CO)$_2$(PMe_3)$_2$(Tp)] (**1Cl***).

Having considered the effect of the (Tp*)(CO)$_2$W≡C– unit upon the platinum centre, it is then useful to consider the effect of the 'PtL$_n$' fragment on the tungsten if we are indeed to view Class **B** carbido complexes as 'metallacarbynes'. Infrared data arising from metal carbonyl complexes have long been employed as an indirect means of determining the π-basicity of a particular metal centre. Variation in the nature of co-ligands impacts on the ν_{CO} frequencies arising from CO-ligands allowing such effects to be quantified, the most celebrated example being the Tolmann electronic parameter for phosphines derived from data for their 'Ni(CO)$_3$' complexes.[11] The '(Tp*)(CO)$_2$M' (M = Mo, W) metal-ligand fragments have proven exceptionally valuable in the development of group 6 metal carbyne chemistry, resulting in a copious body of ν_{CO} data.[12] Table 2 collates data for a selection of carbyne complexes [M(≡CR)(CO)$_2$(Tp*)] with a variety of carbyne substituents, R, spanning electronegative or electropositive, and positively or negatively mesomeric substituents. For simplicity, the two ν_{CO} values have been condensed to the singular Cotton-Kraihanzel force constant for an octahedral *cis*-dicarbonyl complex.[13] We note, perhaps not surprisingly, that these correlate with the σ_p Hammett parameter[14] (R = 0.971, Figure 3) but less well with the σ_m parameter (R = 0.810) consistent with the dominant importance of mesomeric effects. Table 2 also includes carbido complexes to be described herein in addition to Templeton's iron complex [MoFe(μ-C)(CO)$_4$(Tp*)(η-C_5H_5)][2b] with the caveat that there will be a

degree of coupling of Fe–CO and Mo–CO oscillations. This selection does, in passing, highlight the dearth of negatively mesomeric carbyne substituents as a challenge for future investigation. For the carbido complexes considered here, the value for k_{CO} falls in the range 14.42-15.01 Ncm^{-1}, consistent with derived σ_p constants in the range –0.1 to –0.5, and indicating that metal-ligand fragments 'singly' bound to the carbido carbon are indeed positively mesomeric (retrodative, π-basic) to an extent comparable to an amino substituent. These experimental observations therefore reflect the partial π-delocalisation of molecular orbitals along the M–C≡W spine (Figure 2). Within the μ-carbido complexes to be described, it is also apparent that the sub-set of cationic examples are characterised by an increase in k_{CO} which in turn reflects a decrease in retrodonation from platinum, consequently transmitted to the tungsten centre.

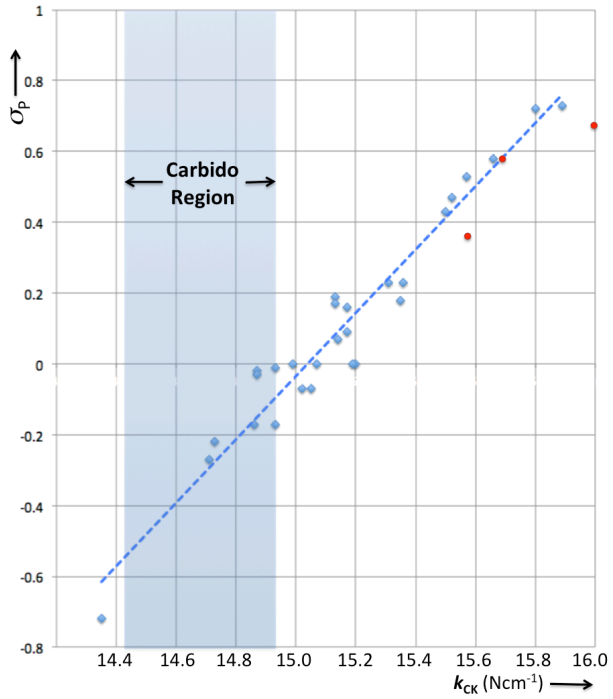

Figure 3. Correlation of the Hammett parameter σ_p with the Cotton-Kraihanzel dicarbonyl force constant k_{CO} for selected complexes of the form [M(≡CR)(CO)$_2$(Tp*)] (M = Mo, W). Molybdenum complexes shown in red but excluded from regression analysis (blue dotted line).

Table 3. Selected infrared data[a] for carbyne complexes of the form [M(≡CR)(CO)$_2$(Tp*)] (M = Mo, W)[12,15-31]

M	R	ν_1(CO) [cm^{-1}]	ν_1(CO) [cm^{-1}]	k_{CK} [Ncm^{-1}]	$\sigma_m^{14}\sigma_p^{14}$	
Mo	CN[15]	2026	1951	15.97	+0.56	+0.66
W	PPh_3^+ [16]	2026	1940	15.89	+0.74	+0.73
W	PEt_3^+ [17x]	2020	1935	15.80	+0.74	+0.73
Mo	DMAP$^+$ [18]	2012	1929	15.66	+0.62	+0.58[e]
Mo	C(=S)NMe_2[19]	2006	1925	15.58	+0.30	+0.34[f]
W	P(=O)Ph_2[20]	2004	1915	15.57	+0.38	+0.53
W	P(=S)Ph_2[20]	2004	1916	15.52	+0.29	+0.47
W	C(=O)Ph[21]	1999	1918	15.50	+0.34	+0.43
W	Br[5]	1994	1905	15.36	+0.39	+0.23
W	I[21]	1992	1907	15.35	0.35	0.18
W	H[21]	1992	1903	15.32	0.00	0.00
W	Cl[5]	1991	1902	15.31	+0.37	+0.23
W	$SnMe_3$[2g]	1979	1902	15.19	0.00	0.00[g]
W	$AsPh_2$[22]	1983	1892	15.17	+0.03	+0.09
W	C≡CPh[23]	1982	1893	15.17	+0.14	+0.16
W	$SiMe_2Ph$[17]	1982	1889	15.14	+0.04	+0.07
W	PPh_2[20]	1982	1891	15.13	+0.11	0.19
W	C_5H_4N-2[24]	1981	1889	15.13	+0.33	0.17
W	TeMe[25]	1977	1886	15.07	0.01	0.00[h]
W	$SiMe_3$[21]	1976	1884	15.05	-0.04	-0.07
W	CH(Ph)OH[21]	1976	1870	15.02	+0.08	-0.07[i]
Mo	**PdBr(dppe)[2k]**	**1971**	**1884**	**15.01**		
W	SMe[17]	1975	1880	14.99	+0.15	0.00
W	Ph[26]	1969	1876	14.93	+0.06	-0.01
W	$CH_2{}^tBu$[27]	1969	1875	14.93	-0.05	-0.17
W	**[Pt(phen)(PPh_3)]$^+$ [9]$^+$**	**1968**	**1874**	**14.91**		
W	**[Pt(bipy)(PPh_3)]$^+$ [10a]$^+$**	**1967**	**1875**	**14.91**		
W	**[Pt(NCMe)(PPh_3)$_2$]$^+$ [4]$^+$**	**1967**	**1872**	**14.89**		
W	OPh[16]	1967	1870	14.87	+0.25	-0.03
W	CH=CHPh[28]	1969	1867	14.87	+0.05	-0.02
W	Me[29]	1968	1867	14.86	-0.07	-0.17
Mo	**PtBr(PPh_3)$_2$[2k]**	**1962**	**1873**	**14.86**		
W	**PdBr(PPh_3)$_2$**	**1957**	**1865**	**14.76**		
W	NPh_2[22]	1960	1859	14.73	0.00	-0.22
W	OMe[b,30]	1958	1862	14.71	+0.12	-0.27
Mo	**Fe(CO)$_2$(η-C_5H_5)[2b]**	**1947**	**1865[d]**	**14.68**		
W	**[Pt(terpy)]$^+$ [8]$^+$**	**1954**	**1858**	**14.68**		
W	**AuPEt$_3$[2g]**	**1951**	**1856**	**14.64**		
W	**PtBr(dppe)**	**1950**	**1856**	**14.63**		
W	**Pt(Tp*)(PPh_3) (12)**	**1947**	**1854**	**14.59**		
W	**Pt(Bp*)(PPh_3) (11)**	**1946**	**1853**	**14.58**		
W	**PtBr(PPh_3)$_2$[2k]**	**1945**	**1854**	**14.59**		
W	**Pt{$H_2B(mt^{Me})_2$}(PPh_3) (13)**	**1940**	**1848**	**14.49**		
W	**NiCl(PEt_3)$_2$[2d]**	**1936**	**1843**	**14.42**		
W	**Pt(S_2CNEt_2)(PPh_3) (7)**	**1935**	**1843**	**14.42**		
W	NEt_2[31]	1936	1833	14.35	-0.23	-0.72

[a]Unless otherwise indicated, data were measured in dichloromethane. [b]Measured in THF. [c] $k_{CK} = 2.0191 \times 10^6 \Sigma(\nu_1^2 + \nu_2^2)$. [d]Fe(CO)$_2$: ν_{FeCO} = 2040, 1991 cm^{-1}. [e]Value for 2,4,6-trimethylpyridinium, [f]Value for CSNHMe; [g]Value for $SnEt_3$. [h]Value for SeMe. [i]Value for CH(Me)OH.

Ligand Substitution Reactions. Notwithstanding the preceding discussion suggesting a comparatively modest *trans*-influence for a Class **B** carbido unit, the bromide ligand in **1** is nevertheless labile and may be abstracted by treatment with silver triflate (AgOTf) in acetonitrile to afford the salt [WPt(μ-C)(CO)$_2$(NCMe)(PPh_3)$_2$(Tp*)]OTf ([**4**]OTf, Scheme 1, Figure 4).

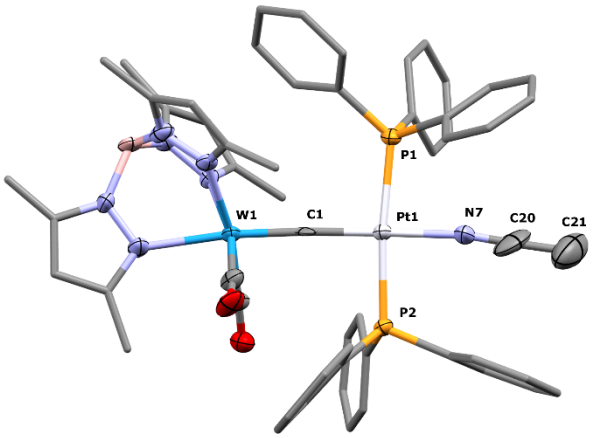

Figure 4. Molecular structure of [**4**]$^+$ in a crystal of **[4]OTf**.2(MeCN) (50% displacement ellipsoids, pyrazolyl and phenyl groups simplified, hydrogen atoms, OTf^- counter-anion and solvent omitted for clarity. Due to an imprecise structural model (R_1= 0.064), caution should be exercised in over-interpreting the data beyond connectivity confirmation. Selected bond lengths (Å), angles (°) and torsions (°): W1–C1 1.839(7), C1–Pt1 1.932(7), W1–C1–Pt1 177.3(5), Pt1–N7 2.051(6), N7–C20 1.20(2), C20–C21 1.45(3), Pt1–P1 2.345(3), Pt–P2 2.325(3), B1–W1–Pt1–P1 2.0(3).

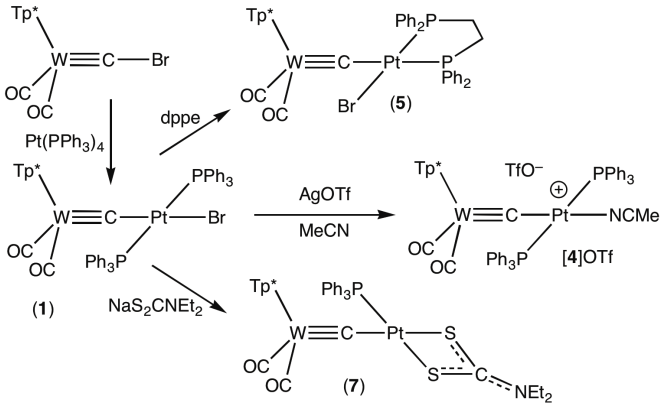

Scheme 1. Synthesis and ligand substitution reactions of **1**.

Although the reaction was essentially spectroscopically quantitative, manipulations to eventually acquire crystalline material resulted in a rather modest isolated yield (33%). Accordingly, if required for synthetic purposes, this material is best generated *in situ*, with the acetonitrile solution being filtered to remove precipitated AgCl, and then used directly. The comparable spectroscopic data associated with the 'Pt(PPh_3)$_2$' and W(CO)$_2$ units (Tables 3-4; ν_{CO}, δ_{Pt}, δ_P, $^1J_{PtP}$, $^2J_{PP}$) are not much changed from those of the precursor **1**. The carbido resonance however, which appears at δ_C = 300.1, is shifted *ca* 19 ppm upfield from that of **1**, presumably reflecting the relative π-donor capacities of bromide and nitrile ligands. The cationic charge at platinum impacts on the electronic nature of the tungsten terminus (reduced π-basicity) in that the frequencies of the carbonyl infrared absorptions (CH_2Cl_2: 1967, 1872 cm^{-1}) are increased from those of the precursor **1** (CH_2Cl_2: 1945, 1852 cm^{-1}).

Table 4. Selected structural and spectroscopic data for platinum carbido complexes (Tp*)(CO)$_2$M≡C–PtL$_n$ (M = Mo, W) described herein.

M	PtL_n	W≡C [Å]	C–Pt [Å]	W–C–Pt [°]	δ_C ppm
W	$PtBr(PPh_3)_2$ (**1**)[2j]	1.856(6)	1.934(6)	169.2(3)	318.6
W	$[Pt(NCMe)(PPh_3)_2]^+$ [**4**]$^+$	1.839(7)	1.932(7)	177.3(5)	300.1
W	PtBr(dppe) (**5**)	1.833(5)	1.990(6)	172.7(4)	356.7
Mo	PtBr(dppe) (**6**)	1.818(5)	1.981(6)	167.9(3)	377.1
W	$Pt(S_2CNEt_2)(PPh_3)$ (**7**)	1.843(4)	1.947(4)	167.1(2)	338.4
W	$[Pt(terpy)]^+$ [**8**]$^+$	1.835(5)	1.938(5)	176.3(3)	367.7
W	$[Pt(bipy)(PPh_3)]^+$ [**10a**]$^+$	1.820(5)	1.960(6)	164.5(4)	325.8
W	$[Pt(tpbby)(PPh_3)]^+$ [**10b**]$^+$	1.839(5)	1.945(5)	168.2(2)	329.6
W	$Pt(Bp^*)(PPh_3)$ (**11**)	1.835(7)	1.963(7)	175.3(6)	338.3
W	$Pt(Tp^*)(PPh_3)$ (**12**)	1.861(2)	1.954(2)	175.2(1)	333.5
W	$Pt\{H_2B(mt^{Me})_2\}(PPh_3)$ (**13**)	1.83(1)	1.97(1)	166.9(7)	328.8

The phosphine ligands in *trans*-**1** are also prone to substitution as indicated by the slow reaction with 1,2-bis(diphenylphosphino)ethane (dppe) which proceeds in toluene over 4 hours at 70 °C to afford the sparingly soluble complex [WPt(μ-C)Br(CO)$_2$(dppe)(Tp*)] (**5**). The *cis*-geometry enforced by the dppe chelate places one phosphine donor *trans* to the carbido carbon such that a large *trans*-$^2J_{PC}$ coupling (74 Hz) is observed for the carbido resonance, which appears downfield (δ_C = 356.7) of the precursor. Perhaps surprisingly, the molecular structure of **5** in the solid state (Figure 6) indicates that the Tp* ligand orients in such a way as to cradle one phosphine phenyl group rather than residing adjacent to the sterically unimposing bromide ligand. This may suggest that interactions between the phenyl and pyrazolyl groups may well be favourable (*vide infra*). The Pt–Br bond length of (2.4746(9) Å), is considerably shorter (66 e.s.d.) than that for the precursor **1** (2.5274(7) Å) indicating that the phosphine exerts a poorer *trans* influence than the carbido ligand. The other phosphine does, however, as expected exert a stronger *trans* influence on the carbido with the Pt–C bond length increasing significantly from 1.934(6) Å in **1** to 1.980(6) Å in **5**. The corresponding molybdenum-platinum carbido complex [MoPt(μ-C)Br(CO)$_2$(dppe)(Tp*)] (**6**) could be similarly obtained from [MoPt(μ-C)Br(CO)$_2$(PPh_3)$_2$(Tp*)][2j,k] with dppe, but in this case the reaction proceeded, albeit slowly (16 hours), at room temperature. Spectroscopic and structural data for **6** are essentially comparable to those for **5** and do not call for further comment.

With the lability of both the bromide and phosphine ligands demonstrated, attention next turned to chelate ligands. Dithiocarbamates are strongly *cis*-chelating and strongly π-basic ligands that are usually though not exclusively innocent in their co-ligand behaviour,[32] with a small number of coupling reactions having been observed between dithiocarbamate and C_1 ligands including carbene,[33] carbyne,[34] vinylidene, allenylidene,[35] cyanide[36] and CS_2 (most likely via thiocarbonyl formation)[37] co-ligands. A small number of 4-

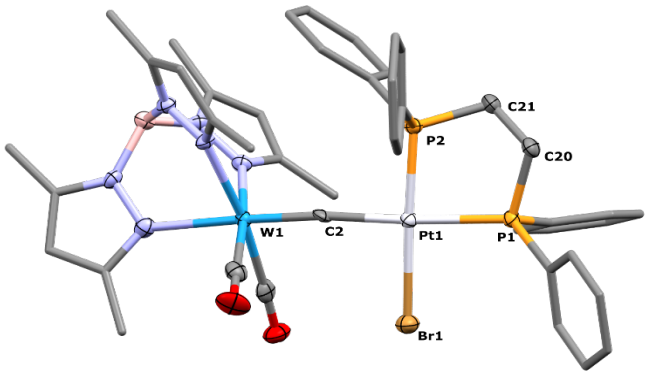

Figure 5. Molecular structure of **5** in a crystal of **5**.$(MeCN)_2$ (50% displacement ellipsoids, hydrogen atoms and solvent omitted, pyrazolyl and phenyl groups simplified). Selected bond lengths (Å) and angles (°): W1–C1 1.833(5), C1–Pt1 1.990(6), Pt1–Br1 2.4746(9), Pt1–P1 2.331(1), Pt1–P2 2.225(2), W1–C1–Pt1 172.7(4), P1–Pt1–P2 85.43(6).

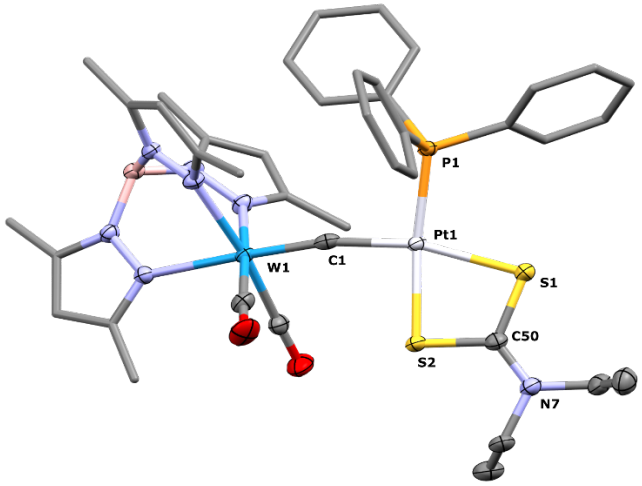

Figure 6. Molecular structure of **7** in a crystal (50% displacement ellipsoids, hydrogen atoms omitted, pyrazolyl and phenyl groups simplified). Selected bond lengths (Å), and angles (°): W1–C1 1.843(4), C1–Pt1 1.947(4), W1–C1–Pt1 167.1(2), Pt1–P1 2.2619(9), Pt1–S1 2.4166(8), Pt1–S2 2.345(1) S1–Pt1–S2 74.05(3), S1–C50–S2 112.1(2).

coordinate organoplatinum(II) examples are known that include structurally characterised complexes such as, *e.g.*, $[Pt(CH_2{}^iPr)(S_2CNEt_2)(PEt_3)]$[38a] and $[Pr(CHMeEt)(S_2CNMe_2)(PCy_3)]$[38b] in addition to a range of derivatives of cyclometalled organyls of less direct comparative use here.

Heating **1** in toluene under reflux for 4 hours with $Na[S_2CNEt_2].2H_2O$ provides the yellow complex $[WPt(\mu\text{-}C)(\kappa^2\text{-}S_2CNEt_2)(PPh_3)(Tp^*)]$ (**7**, Scheme 1). Retention of one phosphine ligand was confirmed by the appearance of a single resonance at δ_P = 13.7 in the $^{31}P\{^1H\}$ NMR spectrum, straddled by satellites due to the ^{195}Pt isotopomer with a $^1J_{PtP}$ coupling of 3880 Hz consistent with this phosphine bound to four-coordinate platinum. The carbido resonance appears as a doublet at δ_C = 338.4 showing a small coupling (6 Hz) consistent with coordination *cis* to the phosphine. Consistent with the characteristic N-C multiple bond character and attendant restricted rotation typical of dithiocarbamates, two distinct ethyl resonance sets are observed in both the ^1H and $^{13}C\{^1H\}$ NMR spectra. The coordination geometry was further confirmed by a crystallographic study (Figure 6) which, as with **5**, involves mutually adjacent ('*syn*') coordination of phosphine and Tp* ligands rather than the alternative *anti* geometry which might have been anticipated based purely on steric grounds. The small chelate bite (S1–Pt1–S2 = 74.05(3)°) demonstrates again that the carbido group exerts a stronger *trans*-influence than does the phosphine with Pt1–S1 2.4166(8) (*trans* to the carbido) being significantly longer than Pt1–S2 2.345(1) (*trans* to the phosphine).

We recently discussed the synthesis of tungsten-platinum μ-carbido complexes *via* the alternative strategy of exploiting the nucleophilicity of Templeton's lithiocarbyne complex $[W(\equiv CLi)(CO)_2(Tp^*)]$[21,39] in halide metathesis reactions with $[PtCl(terpy)]PF_6$ (terpy = 2,2':6',2''-terpyridinyl) or $[PtCl_2(o\text{-}phen)]$.[2l] Whilst the former proceeded without issue to provide $[WPt(\mu\text{-}C)(CO)_2(terpy)(Tp^*)]PF_6$ ($[\mathbf{8}]PF_6$), the latter was complicated by additional attack at the coordinated phenanthroline to provide an unusual metallo-ligand phananthroline-functionalised carbyne.[40]

Ligand substitution reactions commencing with **1** provide a more convenient and generally reliable method for the installation of bi- and tridentate polypyridyl ligands. Thus **1** reacts with terpy and $NaPF_6$ in a polar solvent mixture (CH_2Cl_2/MeOH) at room temperature to provide, following column chromatography, the intensely purple salt $[\mathbf{8}]PF_6$ in 25% yield. While this yield is inferior to that obtained via the salt metathesis approach,[2l] it does demonstrate the useful principle of synthetic divergence from a late synthetic intermediate, *i.e.*, many alternatives to terpy are available without the need to pre-isolate platinum complexes thereof (parallel-linear approach), as shown below.

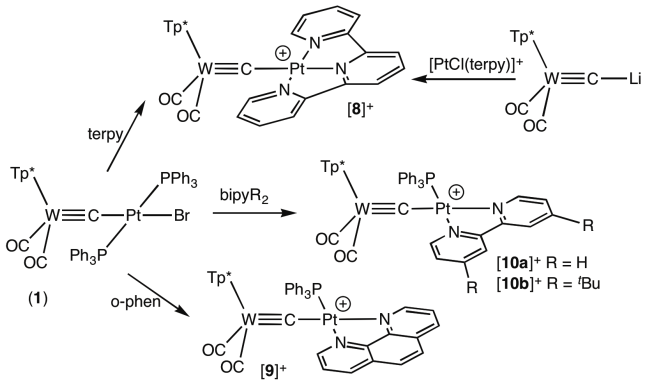

Scheme 2. Synthesis of poly(pyridyl) carbido complexes.

Treating **1** with 1,10-phenanthroline and $NaPF_6$ in a mixture of CH_2Cl_2 and methanol at room temperature for 16 hours affords, after column chromatography, the brown salt $[\mathbf{9}]PF_6$. The phenathroline chelate requires that the carbido and phosphine ligands are mutually *cis*-coordinated such that steric obstruction once again results in the isolation of two inseparable isomers (1:5 ratio) with respect to the two metal termini. Although crystallographic grade crystals were not forthcoming, similar reactions were observed with 2,2'-bipyridyl and 2,2'-bi(4-*tert*.butylpyridyl) to afford the salts $[WPt(\mu\text{-}C)(bipy\text{-}4,4'\text{-}R_2)(PPh_3)(Tp^*)]PF_6$ (R = H **10a** Figure 7, ^{t}Bu

10b, Figure 8, Scheme 3) which in each case was structurally characterised. Whilst [**10a**]PF_6 appears to form as a single isomer within spectroscopically determinable limits ($^{31}P\{^1H\}$ NMR) as with [**9**]PF_6, and for no obvious reason given that the steric variation is remote from platinum, the salt [**10b**]PF_6 exists as two inseparable rotational isomers in the approximate ratio of 1:5.

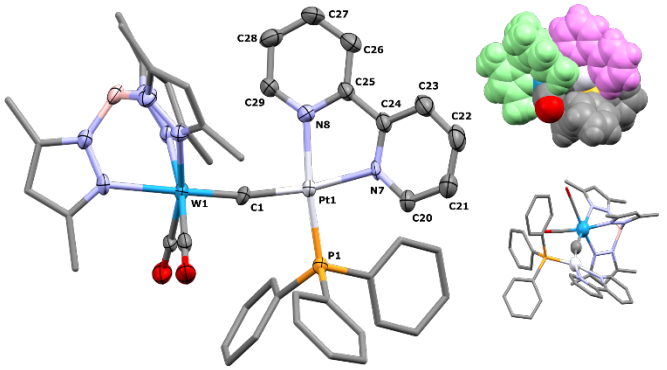

Figure 7. Molecular structure of [**10a**]$^+$ in a crystal of [**10a**]PF_6.$(CHCl_3)_2$ (50% displacement ellipsoids, hydrogen atoms, solvent and PF_6^- counter-anion omitted for clarity. Pyrazolyl and phenyl groups simplified). Selected bond lengths (Å) and angles (°): W1–C1 1.820(5), C1–Pt1 1.960(6), W1–C1–Pt1 164.5(4), Pt1–P1 2.233(2), Pt1–N7 2.142(5), Pt1–N8 2.104(6), N7–Pt1–N8 77.2(2). Inset = space-filling representation demonstrating steric clash between *tris*-pyrazolyl (green) and bipyridyl (cerise) ligands in addition to view along W1–C1–Pt1 vector.

In the preceding discussion it was noted that a recurrent feature of the crystallographic investigations for **1**, [**4**]$^+$, **5** and **7** was the nestling of one phosphine phenyl substituent in the cleft between two pyrazolyl groups on the adjacent Tp* ligand. In the case of [**10a**]$^+$ (Figure 6) and [**10b**]$^+$ (Figure 7) it is the bipyridyl ligand that is preferentially directed towards this cavity. This is most likely because of its tidy co-planarity with the platinum coordination plane that approximately includes the WC unit and unique pyrazolyl group, whilst a symmetrical alignment of a phosphine phenyl group between the pyrazolyl wings is not possible due to the intrinsic local C_3-propellar geometry of the PPh_3 ligand. Thus in both structures the modest W–C–Pt bending actually brings the bipyridyl group *closer* to the Tp* cleft.

Anionic scorpionates. Trofimenko's poly(pyrazolyl)borate scorpionate ligands[41] have played a highly valued supporting role in the development of organometallic chemistry and that is certainly the case for group 10 metals.[42] With a predisposition towards enforcing octahedral or tetrahedral geometries,[43] the Tp[44]and Tp*[45] ligands have proven especially useful for supporting d^6-platinum(IV) six-coordinate geometries. For the more familiar d^8-platinum(II) oxidation state, the square-planar geometry prevails, for which the tridentate Tp or Tp* ligands are clearly *not* best suited, such that reduced denticity is typically encountered. In parallel studies of Class **A** dimetallacumulene carbido complexes[1k] we have observed that the dirhodium species $[Rh_2(\mu\text{-}C)Cl_2(PPh_3)_4]$

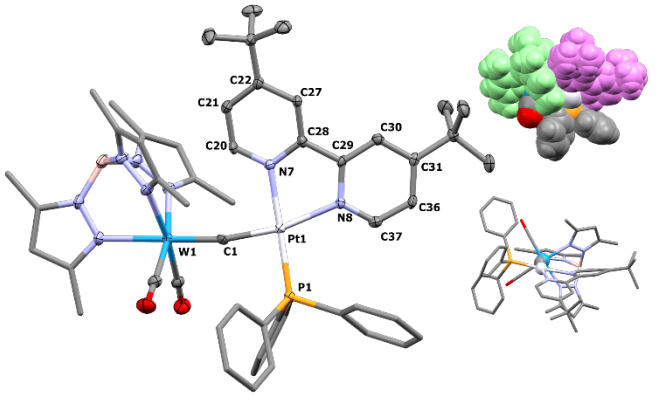

Figure 8. Molecular structure of [**10b**]$^+$ in a crystal of [**10b**]PF_6 (50% displacement ellipsoids, hydrogen atoms and PF_6^- counter-anion omitted, pyrazolyl and phenyl groups simplified for clarity). Selected bond lengths (Å) and angles (°): W1–C1 1.839(5), C1–Pt1 1.945(5), W1–C1–Pt1 168.2(2), Pt1–P1 2.246(1), Pt1–N7 2.101(3), Pt1–N8 2.149(3), N7–Pt1–N8 76.1(1). Inset = space-filling representation demonstrating steric clash between *tris*-pyrazolyl (green) and bipyridyl (cerise) ligands in addition to view along W1–C1–Pt1 vector.

reacts with K[Bp] and K[Bp*] to afford simple symmetrical d^8,d^8-square-planar derivatives $[Rh_2(\mu\text{-}C)(PPh_3)_2(\kappa^2\text{-}Bp)_2]$ (Bp = dihydrobis(pyrazolyl)borate) and $[Rh_2(\mu\text{-}C)(PPh_3)_2(\kappa^2\text{-}Bp^*)_2]$ (Bp* = dihydrobis(dimethylpyrazolyl)borate). Similar treatment with K[Tp] affords the complex $[Rh_2(\mu\text{-}C)(PPh_3)_2(\kappa^3\text{-}Tp)_2]$ in which both rhodium centres adopt trigonal bipyramidal geometries to accommodate the facial-κ^3-Tp ligands. In the case of K[Tp*], however, one phosphine is lost from one rhodium which is thereby precluded from relaxing to a square planar geometry. Accordingly, C–H activation of an adjacent phosphine phenyl group occurs to deliver the mixed oxidation state carbido complex d^8,d^6-$[Rh^IRh^{III}(\mu\text{-}C)H(\mu\text{-}C_6H_4PPh_2\text{-}2)(Tp^*)_2]$. Comparing rhodium and platinum, oxidation of Rh^I to Rh^{III} is rather more facile than Pt^{II} to Pt^{IV}. Furthermore, for 4d and 5d metals, monovalent (d^8) group 9 metal centres more readily adopt 5-coordinate geometries than do divalent group 10 (d^8) metals. With these ligative traits in mind, we therefore considered the installation of scorpionate ligands to platinum carbido derivatives of **1**. Complex **1** reacts with either K[Bp*] or K[Tp*] in refluxing dicholoromethane to provide the complexes $[WPt(\mu\text{-}C)(CO)_2(PPh_3)(Bp^*)(Tp^*)]$ (**11**, Figure **9**, Scheme 3) and (in abysmal yield) $[WPt(\mu\text{-}C)(CO)_2(PPh_3)(Tp^*)_2]$ (**12**, Figure 10). Complex **11** exists at room temperature as a *ca* 1:1 mixture of rotamers that presumably involve either a phosphine phenyl or a pyrazolyl on the Bp* ligand locked between two pyrazolyl groups on the adjacent tungsten bound Tp* ligand. Although B–H···M 3-centre, 2-electron bonding is a common feature of the coordination chemistry of the Bp* ligand[46] the BH···Pt distance observed for **11** (3.07Å) in the solid state is beyond any significant interaction, *e.g.,* $[PtMe_3\{\kappa^3\text{-}H,N,N'\text{-}Bp^*)]$,[47a] $[PtMe_3\{\kappa^3\text{-}H,S,S'\text{-}Bm)]$[47b] and $[Pt_2Me_6I\{\mu\text{:}\kappa^2\text{-}S,S',\kappa^3\text{-}H,S,S'\text{-}Bm)]$ (Bm = dhydrobis(methimazolyl)borate)[47b] have BH···Pt = 1.952, 1.827 and 1.888 Å, respectively. There is similarly no spectroscopic indication (IR, ^1H NMR) that any such association operates in solution.

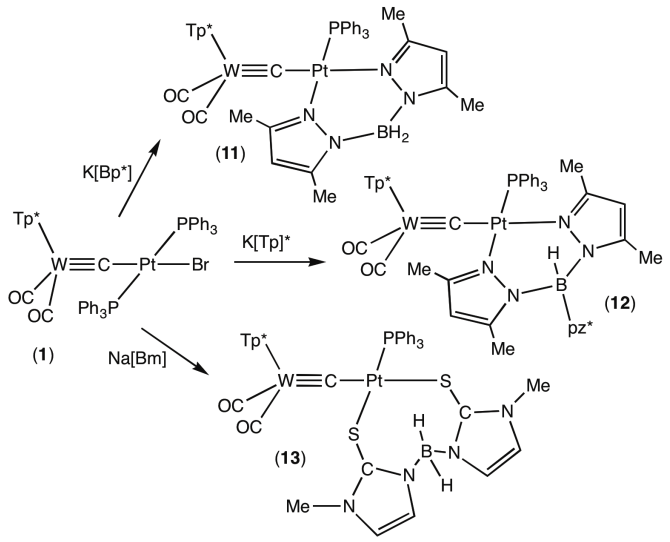

Scheme 3. Synthesis of scorpionate carbido complexes (pz* = 3,5-dimethylpyrazol-1-yl).

It should be noted that for the isomer with interlocked Tp* and Bp* ligands, inversion of the C_1-symmetrc L'LPtBp* 'boat' through a C_s-symmetric transition state would interconvert enantiomers but *not* provide a means for the Bp* pyrazolyl groups to exchange sites.

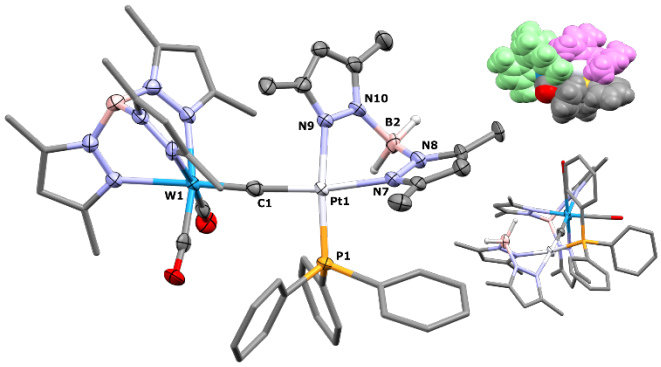

Figure 9. Molecular structure of **11** in a crystal of **11**.($CHCl_3$) (50% displacement ellipsoids. Hydrogen atoms and solvent omitted for clarity. Spectator pyrazolyl and phenyl groups simplified). Selected bond lengths (Å) and angles (°): W1–C1 1.835(7), C1–Pt1 1.963(7), W1–C1–Pt1 175.3(6), Pt1–P1 2.256(3), Pt1–N7 2.138(6), Pt1–N9 2.111(9), N7–Pt1–N9 81.6(3), Pt1···H2A 3.06(9). Inset = space-filling representation demonstrating steric clash between Tp* (green) and Bp* (cerise) ligands in addition to view along W1–C1–Pt1 vector showing large Pt1···H2A distance.

In the case of **12**, the borate also adopts a bidentate rather than tridentate κ^3-*N,N'N"* or κ^3-*H,N,N'* coordination mode in the solid state to provide a square planar geometry at platinum (Figure 10). For **12**, as with **11,** it is a pyrazolyl rather than phosphine phenyl group that is recumbent in the tungsten bis(pyrazolyl) cleft. Whilst the difference in Pt–N lengths for **11** is not crystallographically significant, in the case of **12** the pyrazolyl group *trans* to the carbido is significantly (20 e.s.d.) displaced relative to that *trans* to the phosphine.

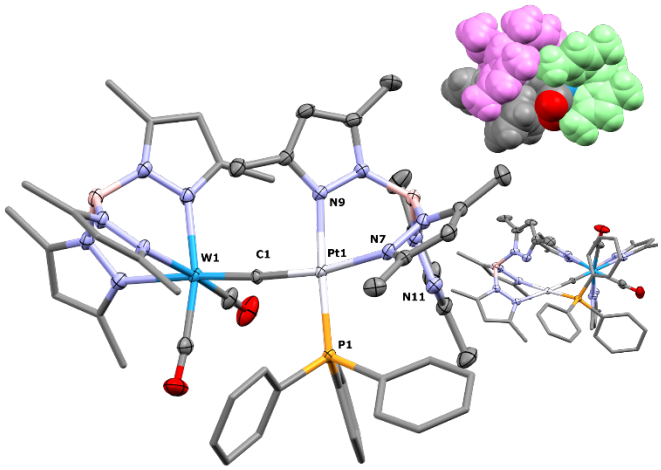

Figure 10. Molecular structure of **12** in a crystal (50% displacement ellipsoids. Hydrogen atoms omitted for clarity. Spectator pyrazolyl and phenyl groups simplified). Selected bond lengths (Å) and angles (°): W1–C1 1.861(2), C1–Pt1 1.954(2), W1–C1–Pt1 175.2(1), Pt1–P1 2.2631(6), Pt1–N7 2.129(2), Pt1–N9 2.090(2), N7–Pt1–N9 81.39(9), Pt1–N11 3.525(3). Inset = space-filling representation demonstrating steric clash between *tris*-pyrazolyl ligands (cerise and green) in addition to view showing pendant pyrazolyl ring.

The poly(2-mercatoimidazol-1-yl)borate class of ligands $H_nB(mt^R)_{4-n}$ (n = 1,2; mt = 2-mercapto-3-R-imidazol-1-yl; R = Me, ^{t}Bu, Ph, $C_6H_2Me_3$-2,4,6) introduced by Spicer, Reglinski[48] and Parkin[49] appear superficially similar to Trofimenko's pyrazolylborates, being sometimes referred to as soft scorpionates.[48b] There are also many divergences between the coordination chemistries of the two ligand classes, not simply due to the soft, σ+π donor nature of the sulphur donors, but also because upon chelation to a metal, the boron is separated by three (N–C–S) rather than two (N–N) atom bridges. Amongst the implications are (i) a propensity to enter into 3-centre, 2-electron B–H···M interactions[46c,50] and in the case of $HB(mt^R)_3$ (n = 1), the adoption of a locally C_3-symmetric (*i.e.*, chiral) $HB(mt^R)_3M$ cage (*cf.* locally C_{3v}-symmetric $HB(pz)_3M$) the inversion of which is typically a high energy process.[51]

Our own interest in the chemistry of these ligands has focused on the ease with which they may undergo B–H activation to provide metallaboratranes[52] which feature a *trans*-annular direct M→B polar-covalent (dative) bond.[53] These are now known for all the metals of groups 8-11 (high d-occupancy being an obvious requirement) including platinum with a variety of heterocycles replacing the original methimazolyl buttresses.[54] In the case of methimazolylborate-derived metallaboratranes the key installation sequence involves geometrically pre-disposed[47b] B–H activation. This is in many but not all cases followed by hydrogen abstraction by either reductive elimination with a co-ligand[52] or extraneous base.[54a] Given that we have recently had reason to implicate deprotonation of a coordinated cyclobutadiene ligand in an intermediate platinum carbido complex,[2l] we considered whether introduction of a dihydrobis(methimazolyl)borate ligand to **1** might result in metallaboratrane formation (Scheme 4). Contrary to expectations, the reaction of **1** with $Na[H_2B(mt^{Me})_2]$ resulted in the rapid formation of $[WPt(\mu\text{-}C)(CO)_2(PPh_3)\{H_2B(mt^{Me})_2\}(Tp^*)]$ (**13**; Bm =

dihydrobis(methimazolyl)borate, Figure 11) in 77 % isolated yield.

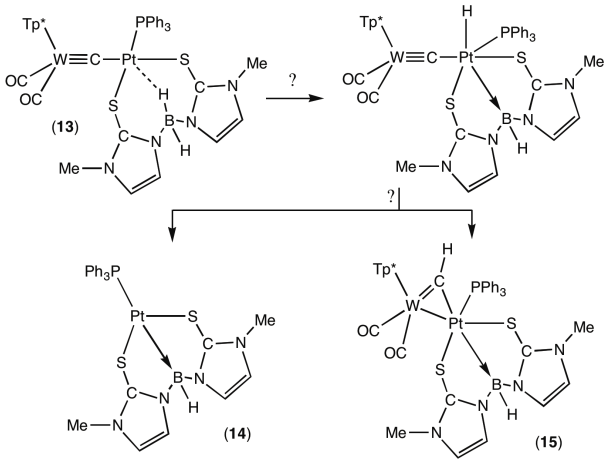

Scheme 4. Suggested relationship between carbido-borate and methylidyne-borane isomers.

Given the normal propensity for platinaboratrane formation, the isolation of **13** as the first stable organometallic platinum(II) complex of this ligand class is notable (*cf.* Pt^{IV}: $[PtMe_3\{\kappa^3\text{-}H,S,S'\text{-}H_2B(mt^{Me})_2\}]$[47b]), with no indication of reductive elimination to form $[Pt(PPh_3)\{\kappa^3\text{-}B,S,S'\text{-}H_2B(mt^{Me})_3]$ (**14**) or its putative methylidyne adduct precursor (**15**). Whilst **14** was and remains unknown, it would be closely related to the isolable platinaboratrane $[Pt(PPh_3)\{\kappa^3\text{-}B,S,S'\text{-}HB(pyS)_2\}]$ described by Owen[54h] which arises from the reaction of $[Pt_2(\sigma,\eta^2\text{-}C_8H_{11}OMe\text{-}8)_2(PPh_3)_2]$ with $Na[H_2B(pyS)_2]$.

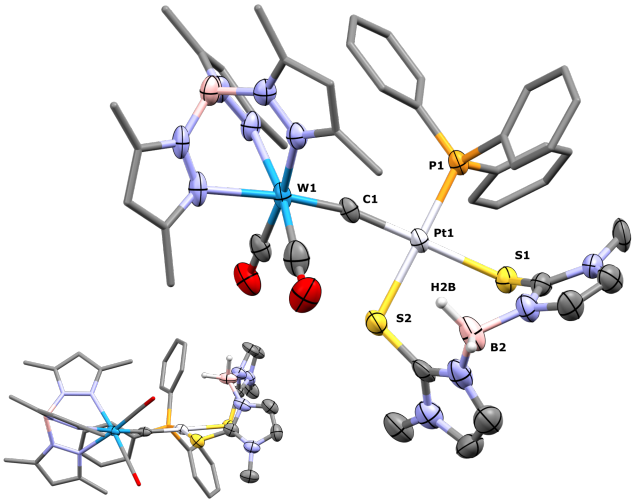

Figure 11. Molecular structure of **13** in a crystal of **13**.($CHCl_3$) (50% displacement ellipsoids. Hydrogen atoms and solvent omitted for clarity. Spectator pyrazolyl and phenyl groups simplified). Selected bond lengths (Å) and angles (°): W1–C1 1.83(1), C1–Pt1 1.97(1), W1–C1–Pt1 166.9(7), Pt1–P1 2.250(3), Pt1–S1 2.455(2), Pt1–S2 2.346(4), S1–Pt1–S2 93.6(1), Pt1–H2B 3.3(2). Inset = view highlighting lack of Pt–H interaction.

The spectroscopic data for **13** are each consistent with its formulation, which was confirmed crystallographically (Figure 11). The ^1H NMR spectrum of **13** is barren to high field of $SiMe_4$, which is indicative of the absence of any enduring B–H···Pt interaction (*cf.* δ_H –3.2 br. and $^1J_{PtH}$ 330 Hz for $[PtMe_3\{\kappa^3\text{-}H,S,S'\text{-}H_2B(mt^{Me})_2\}]$[47b]), consistent with square-planar geometry at platinum. Poly(methimazoly)borate ligands are especially potent π-donors and this is manifest in particularly low frequency ν_{CO}-associated infrared absorptions (1940, 1848 cm^{-1}), being comparable to those for the dithiocarbamate derivative **7**.

Carbido Chemical Shifts – For the complexes investigated, the carbido chemical shift δ_C appears in the region 300-357 ppm, somewhat downfield from those for more conventional carbyne substituents for complexes of the form $[W(\equiv CR)(CO)_2(Tp^*)]$.[12] Since on purely electronegativity grounds, substantial shielding would be expected to be provided by platinum (*cf.* hydrides, alkyls *etc.*). It may therefore be surmised that as with carbyne ligands, there is a significant paramagnetic contribution arising from closely spaced occupied and unoccupied orbitals. Based on the frontier orbitals for hypothetical **1Cl*** (Figure 2), these are associated with the π-component of the W≡C–Pt linkage and accordingly the shielding tensor is highly anisotropic. Taking the W≡C–Pt spine as the *z* axis, the axial component δ_z of the chemical shift tensor makes only a modest contribution to the observed isotropic chemical shift whilst the azimuthal components (δ_x, δ_y) would be expected to dominate, as observed for conventional carbynes.[56] It might therefore be expected that the chemical shift would be responsive to variations in the energies of the π-orbitals associated with the W≡C–Pt spine and accordingly show some correlation with the k_{CO} values which as described above correlate with Hammett σ_P parameters for more conventional substituents. It transpires that this is not the case and we are unable to identify any obvious pattern. We do, nevertheless note that, with the inexplicable exception of **7**, there is a loose correlation (R = 0.948) between the chemical shifts for the carbido (δ_C) and platinum-195 (δ_{Pt}) nuclei (Table 5, Figure 12). The platinum NMR chemical shifts fall in the region typical of square planar platinum(II),[57] and span (by ^{195}Pt standards) a comparatively narrow range (*ca* 400 ppm) given the wide variety of ligand-types.

Table 5. Selected NMR data[a] for μ-carbido complexes of the form [WPt(μ-C)(CO)$_2$(Tp*)L$_n$]

PtL$_n$	δ_C [ppm]	δ_{Pt} [ppm]	δ_P [ppm]	$^2J_{PP}$ Hz	$^1J_{PtP}$ Hz
PtBr(PPh$_3$)$_2$ (**1**)[b]	317.2	-3821	26.25	443	3178
			22.19	443	3200
PtBr(PPh$_3$)$_2$ (**1'**)[b]	318.7	-3718	28.27	443	*c*
			23.91	443	*c*
[Pt(NCMe)(PPh$_3$)$_2$]$^+$ [**4**]$^+$	300.1	-3832	23.29	385	3169
			19.68	385	3093
PtBr(dppe) (**5**)[e]	356.7	*d*	38.10	-	1526
			34.51	-	4068
Pt(S$_2$CNEt$_2$)(PPh$_3$) (**7**)	338.4	-3828	13.68	-	3880
[Pt(phen)(PPh$_3$)]$^+$ [**9**]$^+$	324.7	-3619	15.73	-	4341
[Pt(bipy)(PPh$_3$)]$^+$ [**10a**]$^+$	325.8	-3587	16.37	-	4293
[Pt(tpbby)(PPh$_3$)]$^+$ [**10b**]$^+$	329.6	-3580	16.25	-	4250
Pt(Bp*)(PPh$_3$) (**11**)	338.3	-3495	7.52	-	4285
Pt(Bp*)(PPh$_3$) (**11'**)	332.6	-3477	5.38	-	4161
Pt(Tp*)(PPh$_3$) (**12**)	333.5	-3433	3.07	-	4288
Pt(Bm)(PPh$_3$) (**13**)	328.8	-3561	14.62	-	3979

[a] Unless otherwise indicated, data were measured in $CDCl_3$ at 295 K; [b] Two rotamers **1/1'** or **11/11'** observed. [c] Insufficient signal/noise to ascertain. [d] Insufficiently soluble to identify δ_{Pt}. [e] Measured in CD_2Cl_2.

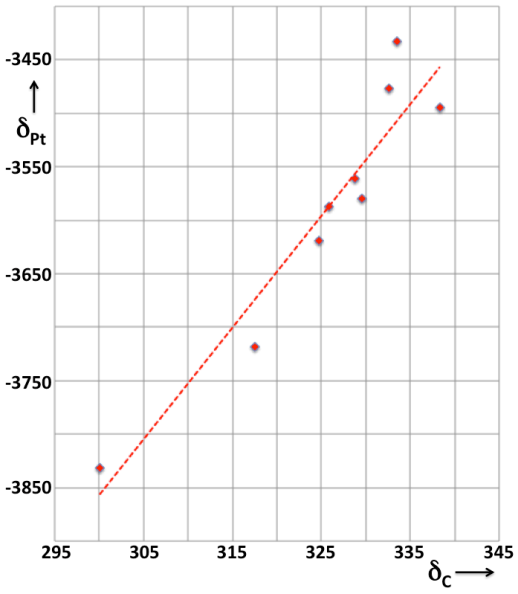

Figure 12. Correlation of δ_C and δ_{Pt} for tungsten-platinum μ-carbido complexes (datum for **7** omitted).

Conclusions

Beginning with the conveniently accessible μ-carbido complex [WPt(μ-C)(CO)$_2$(PPh$_3$)$_2$(Tp*)] (**1**), a range of derivatives are readily available by virtue of the lability of bromide and phosphine ligands bound to the platinum terminus. These substitution reactions proceed with retention of the W≡C–Pt spine and allow substantial variations in the electronic nature of the platinum including charge and π-dative or π-acidic co-ligands that are either monodentate or bidentate. When tridentate ligands are presented, the proclivity for divalent platinum to maintain a four-coordinate square planar geometry prevails. In no instance was ligand substitution observed to occur at the tungsten centre, consistent with its coordinative saturation and strongly bound (low ν_{CO}) carbonyl ligands.

Electronic communication between the platinum and tungsten centres is evidenced by the impact of variations upon the infrared data for tungsten carbonyl ligands, a phenomenon that could be shown, for related carbynes, to correlate with the π-basicity (σ_p Hammett analysis) of the carbyne substituent. While no correlation between k_{CO} and the carbido ^{13}C chemical shift was identified, there was a loose correlation between δ_C and δ_{Pt}. Electronic communication through orbitals of π-symmetry with respect to the W≡C–Pt spine is implicated by computational interrogation of the molecular orbitals of the hypothetical model complexes [WPt(μ-C)X(CO)$_2$(PMe$_3$)$_2$(Tp*)] (X = Cl **1Cl***, Br **1Br***).

The structural *trans* influence of the carbido unit was found to be greater than that for an alkynyl, being intermediate between alkyl and alkenyl ligands. Templeton has estimated the pK_a for [W(≡CH)(CO)$_2$(Tp*)] in THF to be *ca* 28.7(3) which is greater that for simple alkynes [RC≡CH] (R = Ph 23.2; ^{t}Bu 25.5).[58] This may be loosely taken as indicative of the carbido being a stronger σ-donor than σ-alkynyls, however since the pK_a of ethene is *ca* 44 and that of alkanes *ca* 60, there must also be a π-component to the *trans* influence. Numerous facile ligand substitution processes were documented above. In terms of kinetic *trans* effect, the ability of the W≡C– unit to amphoterically serve as a π-donor or π-acceptor (Chart 3 *cf*. Class **A** carbido character) may well contribute to the stabilisation of transition states with reduced (I_d) or increased (I_a) coordination number, respectively.

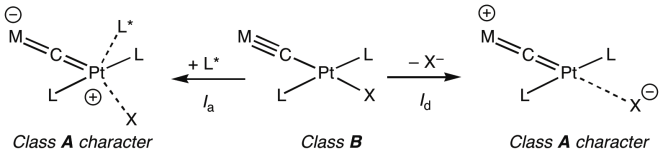

Chart 3. Class **A** carbido stabilisation of dissociative (I_d) or associative (I_a) ligand substitution transition states.

The synthetic approaches outlined here are in principle available to other group 10 *d*^{10} substrates that are amenable to oxidative addition pointing towards an extensive chemistry.

Experimental

General

Experimental work was performed using standard Schlenk techniques using dried and pre-purified nitrogen or in an inert atmosphere glove-box charged with an argon atmosphere unless specified otherwise. Reactions employed dried and degassed solvents distilled over sodium and benzophenone (ethers, arenes and paraffins) or calcium hydride (CH_2Cl_2, MeCN). The compounds [M(≡CBr)(CO)$_2$(Tp*)] (M = Mo, W),[5] [WPt(μ-C)(CO)$_2$(PPh$_3$)$_2$(Tp*)] (**1**)[21] K[Bp*],[41] K[Tp*][41] and Na[Bm][55] were prepared according to published procedures. All other reagents were used as received from commercial suppliers.

NMR spectra were obtained on a Bruker Avance 400 (^1H at 400.1, $^{13}C\{^1H\}$ at 100.6, $^{19}F\{^1H\}$ at 376.5, $^{31}P\{^1H\}$ at 162.0,

^{195}Pt{^{1}H} at 85.7 MHz), a Bruker Avance 600 (^{1}H at 600.0, ^{13}C{^{1}H} at 150.9 MHz) or a Bruker Avance 700 (^{1}H at 700.0, ^{13}C{^{1}H} at 176.1, ^{31}P{^{1}H} at 283.4 MHz) spectrometers at the temperatures indicated. Chemical shifts (δ) are reported in ppm with coupling constants given in Hz and are referenced to the solvent resonance or external references {$CFCl_3$ for ^{19}F{^{1}H}, 85% H_3PO_4 in H_2O for ^{31}P{^{1}H}, 1.2M Na_2PtCl_6 for ^{195}Pt}. The multiplicities of NMR resonances are denoted by the abbreviations s (singlet), d (doublet), t (triplet), m (multiplet), br (broad) and combinations thereof for more highly coupled systems. Where applicable, the stated multiplicity refers to that of the primary resonance exclusive of ^{183}W or ^{195}Pt satellites. In select cases, distinct peaks were observed in the ^{1}H and ^{13}C{^{1}H} NMR spectra, but to the level of accuracy that is reportable (*i.e.*, 2 decimal places for ^{1}H NMR, 1 decimal place for ^{13}C{^{1}H} NMR) they are reported as having the same chemical shift. Phosphorus-31 chemical shifts are reported having, where appropriate, been corrected for roofing effects in AB spin systems.[67] Some compounds contain variable, non-negligible ratios of rotamers, hence absolute assignment of all signals is sometimes not possible.

The abbreviation 'pz' is used to refer to the pyrazolyl rings on the hydridotris(3,5-dimethylpyrazol-1-yl)borate (Tp*) ligand. Spectra provided generally correspond to samples obtained directly from chromatography and may contain residual solvent as recrystallised samples often display reduced solubility. The B*H* protons give rise to very broad signals around 4–5 ppm in the ^{1}H NMR spectra due to coupling to the quadrupolar boron nuclei. These are not listed in the experimental NMR data as their chemical shifts and associated integrals are not determined accurately. The BH unit, being remote from the metal centre of interest is not particularly responsive to variations and accordingly ^{11}B{^{1}H} NMR spectra were not recorded.

Infrared spectra were obtained using a Shimadzu FTIR-8400 spectrometer (liquid) or Perkin Elmer FTIR Spectrum 2 (Solid State ATR, diamond anvil). Signals are denoted according to their absorption strength such as very sharp (vs), strong (s), medium (m), weak (w) or broad (br). Elemental microanalytical data were provided the London Metropolitan University. Solvates evident from data were confirmed where possible by NMR spectroscopy. High-resolution electrospray ionisation mass spectrometry (ESI-MS) was performed by the ANU Research School of Chemistry mass spectrometry service with acetonitrile or dichloromethane as the matrix.

Data for X-ray crystallography were collected with Agilent Xcalibur or SuperNova CCD diffractometers using Mo-Kα radiation (λ = 0.71073 Å) or Cu-Kα radiation (λ = 1.54184 Å) employing the *CrysAlis PRO* software.[59] The structures were solved by direct or Patterson methods and refined by full-matrix least-squares on F^2 using the SHELXS or SHELXT and SHELXL programs.[60] Hydrogen atoms were located geometrically and refined using a riding model. Diagrams were produced using the CCDC visualisation program Mercury.[61]

Computational studies were performed by using the *SPARTAN18* suite of programs.[62] Geometry optimisation (gas phase) was performed at the DFT level of theory using the exchange functional of Becke[63] for **1Cl*** (for consistency with reference 6) and the ωB97X-D functional of Head-Gordon[64] for **1Br***. The Los Alamos effective core potential type basis set (LANL2Dζ) of Hay and Wadt[65] was used for Pt and W Pople 6-31G* basis sets[66] were used for all other atoms. Frequency calculations were performed to confirm that the optimized structure was a minimum and also to identify vibrational modes of interest (ν_{WCPt}). Cartesian atomic coordinates are provided in the electronic supporting information.

Synthesis of [WPt(μ-C)(CO)$_2$(NCMe)(PPh$_3$)$_2$(Tp*)][OTf] [4]OTf.

A solution of [WPt(μ-C)Br(CO)$_2$(PPh$_3$)$_2$(Tp*)] (**1**: 94 mg, 70 µmol) and AgOTf (29 mg, 110 µmol) was stirred in acetonitrile (10 mL). The reaction was complete after 2 hours as indicated by ^{31}P{^{1}H} NMR spectroscopic analysis to provide a grey precipitate and a bright orange supernatant. The supernatant was collected *via* filter cannula and the volatiles were removed under reduced pressure to provide a crude orange semi-crystalline solid (95 mg). The solid was ultrasonically triturated in Et_2O (3 x 10 mL) discarding the decantate each time, providing an orange residual solid. Recrystallisation from MeCN/Et_2O afforded red crystals identified as [**4**]OTf (34 mg, 23 µmol, 33% yield). Crystals thus obtained were found to be suitable for X-ray diffraction analysis. IR (CH_2Cl_2, cm^{-1}): 1967 vs ν_{CO}, 1949 s ν_{CO}, 1872 vs ν_{CO}, 1856 s ν_{CO} (two rotamers, see spectrum in ESI). ^{1}H NMR (400 MHz, $CDCl_3$, 25 °C) δ_H = 7.94 – 7.81 [m, 5 H, C_6H_5], 7.48 [s.br, 8 H, C_6H_5], 7.40 – 7.31 [m, 3 H, C_6H_5], 7.29 – 7.15 [m, 11 H, C_6H_5], 7.14 – 7.02 [m, 7 H, C_6H_5], 6.92 – 6.73 [m, 2 H, C_6H_5], 5.50, 5.42, 5.22 [s x 3, 1 H x 3, pzCH], 2.31, 2.27 [s x 2, 6 H x 2, $pzCH_3$], 2.10, 1.92, 1.84 [s x 3, 3 H x 3, $NCCH_3$ and $pzCH_3$]. ^{13}C{^{1}H} NMR (150 Hz, $CDCl_3$, 25 °C) δ_C = 300.1 [dd, $^{2}J_{CP}$ = 10, 4 Hz, W≡C–Pt], 229.2 [$^{1}J_{CW}$ = 174 Hz, CO], 151.9 150.9 [C^5(pz)], 144.2 143.9 [C^3(pz)], 134.7, 134.4 [d, $^{3}J_{CP}$ = 11 Hz, $C^{3,5}(C_6H_5)$], 131.8, 131.6 [d, $^{4}J_{CP}$ = 3 Hz, $C^4(C_6H_5)$], 129.2, 128.6 [d, $^{2}J_{CP}$ = 11 Hz, $C^{2,6}(C_6H_5)$], 116.5 (Pt–N*C*Me), 106.9, 106.4 [C^4(pz)], 17.2 14.7 12.9 12.5 [$pzCH_3$], 2.01 [NCCH_3]. ^{19}F{^{1}H} NMR (377 MHz, $CDCl_3$, 25 °C) δ_F = –78.0 [O_3SCF_3]. ^{31}P{^{1}H} NMR (161 MHz, $CDCl_3$, 25 °C) δ_P(corrected for roofing[67]) = 23.29 [d, $^{2}J_{PP}$ = 385, $^{1}J_{PPt}$ = 3169 Hz, P_A], 19.68 [d, $^{2}J_{PP}$ = 385, $^{1}J_{PPt}$ = 3093 Hz, P_B]. ^{195}Pt{^{1}H} NMR (85.7 MHz, $CDCl_3$, 25 °C) δ_{Pt} = –3832 [t, $^{1}J_{PtP}$ = 3132 Hz]. MS (ESI, *m/z*): Found: 1268.2900. Calcd for $C_{57}H_{55}BF_3N_7O_5P_2PtSW$ [M-MeCN-H]$^+$: 1268.2883. Anal. Found: C, 46.84; H, 3.80; N, 6.79%. Calcd for $C_{57}H_{55}BF_3N_7O_5P_2PtSW$: C, 46.86; H, 3.81; N, 6.73%. *Crystal data for* $C_{56}H_{55}BN_{7.05}O_2P_2PtW\bullet CF_3O_3S\bullet 2(C_2H_3N)$, M_w = 1541.63, monoclinic, $P2_1/c$, a = 24.2079(16), b = 10.5921(5), c = 26.1839(17) Å, β = 116.111(8)°, V = 6028.7(7) Å^3, Z = 4, ρ_{calc} = 1.699 Mgm^{-3}, μ(Mo $K\alpha$) = 4.38 mm^{-1}, T = 150(0) K, clear light orange block 0.38 × 0.3 × 0.17 mm, 15101 independent measured reflections (θ_{max} = 29.5), R_1 = 0.063, wR_2 = 0.150 for 11224 reflections [$I > 2\sigma(I)$], 786 parameters, 22 restraints. Due to low precision, the .cif for this salt has not been deposited with the CCDC..

Synthesis of [WPt(μ-C)Br(CO)$_2$(dppe)(Tp*)] (5)

A solution of [WPt(μ-C)Br(CO)$_2$(PPh$_3$)$_2$(Tp*)] (**1**: 608 mg, 0.450 mmol) and dppe (178 mg, 0.446 mmol) was heated with stirring in toluene (20 mL) for 4 hours at 70 °C. The initial orange

solution decolourised partially as a yellow solid precipitated. The solvent was removed under reduced pressure and the residue crystallised by slow concentration of a solution in a mixture of CH_2Cl_2 and n-hexane to give a yellow microcrystalline solid. This solid was collected via vacuum filtration and washed with n-hexane (10 mL) before drying *in vacuo* for 4 hours to give **5** as a yellow powder (508 mg, 0.416 mmol, 94% yield). Crystals of an acetonitrile solvate suitable for X-ray diffractometry were grown by vapour diffusion of Et_2O into a solution of **5** in acetonitrile. IR (CH_2Cl_2, cm^{-1}): 1950 vs ν_{CO}, 1856 vs ν_{CO}. ^1H NMR (400 MHz, $CDCl_3$, 25 °C) δ_H = 7.86 – 7.78 [m, 5 H, C_6H_5], 7.71 – 7.64 [m, 5 H, C_6H_5], 7.46 – 7.42 [m, 5 H, C_6H_5], 7.39 [s, 4 H, C_6H_5], 7.17 – 7.05 [m, 5 H, C_6H_5], 5.62 [s, 2 H, pzCH], 5.58 [s, 1 H, pzCH], 2.47, 2.45 [s x 2, 3 H x 2, $pzCH_3$], 2.35 [s, 6 H, $pzCH_3$], 2.28 [s, 3 H, $pzCH_3$], 2.23 [s, 3 H, $pzCH_3$], 2.03 – 1.93 [m, 4 H, PCH_2]. $^{13}C\{^1H\}$ NMR (151 MHz, CD_2Cl_2, 25 °C) δ_C = 356.7 [d.br., $^2J_{CP}$ = 74 Hz, W≡C–Pt], 229.4 [$^1J_{CW}$ = 177 Hz, CO], 152.4 152.0 [C^5(pz)] 145.2 144.3 [C^3(pz)], 134.3 134.1 [d, $^3J_{CP}$ = 11 Hz, $C^{3,5}(C_6H_5)$], 131.9 131.6 [$C^4(C_6H_5)$], 130.8 [d, $^1J_{CP}$ = 45 Hz, $C^1(C_6H_5)$], 129.2 [d, $^2J_{CP}$ = 11 Hz, $C^{2,6}(C_6H_5)$], 128.7 [d, $^2J_{CP}$ = 11 Hz, $C^{2,6}(C_6H_5)$], 106.6, 106.3 [C^4(pz)], 31.3 [s.br., PCH_2], 25.0 [d, $^1J_{CP}$ = 31 Hz, PCH_2], 17.4 15.2 13.1 12.7 [pz*C*H$_3$]. $^{31}P\{^1H\}$ NMR (162 MHz, $CDCl_3$, 25 °C) δ_P = 38.10 [s.br, $^1J_{PPt}$ = 1526 Hz, P *cis* to Br], 34.51 [s.br, $^1J_{PPt}$ = 4068 Hz, C *cis* to C≡W]. Satisfactory $^{195}Pt\{^1H\}$ NMR spectra could not be measured irrespective of solvent or temperature (–60 to +50 °C) due to poor solubility and signal multiplicity. MS (ESI, *m/z*): Found: 1222.1672. Calcd for $C_{44}H_{46}BBrN_6O_2P_2PtW$ $[M+H]^+$: 1222.1665. Anal. Found: C, 46.05; H, 4.74; N, 6.28%. Calcd for $C_{44}H_{46}BBrN_6O_2P_2PtW$: C, 46.13; H, 4.69; N, 6.38%. *Crystal data for* $C_{44}H_{46}BBrN_6O_2P_2PtW\bullet2(C_2H_3N)$, M_w = 1304.57, monoclinic, $P2_1$, *a* = 12.1891(1) Å, *b* = 10.5285(1) Å, *c* = 19.6792 (1) Å, β = 108.011 (1)º, *V* = 2401.73 (4) Å^3, *Z* = 2, ρ_{calc} = 1.804 Mgm^{-3}, μ(Cu *K*α) = 11.71 mm^{-1}, *T* = 150(0) K, clear light orange needle 0.24 × 0.11 × 0.04 mm, 9573 independent measured reflections (θ_{max} = 73.9 °), R_1 = 0.027, wR_2 = 0.073 for 9520 reflections [$I > 2\sigma(I)$], 588 parameters, 2 restraint. CDCC 1997712.

Synthesis of [MoPt(μ-C)Br(CO)$_2$(dppe)(Tp*)] (6)

The compounds [MoPt(μ-C)Br(CO)$_2$(PPh_3)$_2$(Tp*)] (92 mg, 73 μmol) and dppe (37 mg, 93 μmol) were dissolved in toluene (10 mL) to afford a yellow solution. Stirring for 16 hours resulted in formation of a yellow suspension. The solvent was removed *via* rotary evaporation to give a yellow solid. This was purified by anaerobic flash column chromatography (silica gel, gradient elution). A bright yellow band was eluted with neat CH_2Cl_2 and was subsequently crystallised from a mixture of CH_2Cl_2 and *n*-hexane to give a yellow powder. This was collected *via* vacuum filtration, washed with *n*-pentane and dried *in vacuo* for 4 hours to give **6** (74 mg, 65 μmol, 89% yield). IR(CH_2Cl_2, cm^{-1}): 1965 vs ν_{CO}, 1876 vs ν_{CO}. ^1H NMR (400 MHz, $CDCl_3$, 25 °C, δ): 7.82 [m, 5 H, C_6H_5], 7.67 [m, 5 H, C_6H_5], 7.44 [m, 5 H, C_6H_5], 7.11 [m, 5 H, C_6H_5], 5.62 [s, 2 H, pzCH], 5.58 [s, 1 H, pzCH], 2.47 [s.br., 6 H, $pzCH_3$], 2.35 [s, 6 H, $pzCH_3$], 2.28, 2.23 [s x 2, 3 H x2 , $pzCH_3$], 1.97 [m, 4 H, P*CH*$_2$]. $^{13}C\{^1H\}$ NMR (151 MHz, CD_2Cl_2, 25 °C) δ_C = 377.1 [d.br., $^2J_{CP}$ = 77 Hz, Mo≡*C*–Pt], 231.5 [CO], 151.5, 151.3 [C^5(pz)], 145.1, 144.3 [C^3(pz)], 134.3, 134.1 [d, $^2J_{CP}$ = 11 Hz, $C^{2,6}(C_6H_5)$], 132.0, 131.7 [$C^4(C_6H_5)$], 130.6 [d, $^1J_{CP}$ = 46 Hz, $C^1(C_6H_5)$], 129.3 [d, $^3J_{CP}$ =10 Hz, $C^{3,5}(C_6H_5)$], 128.7 [d, $^3J_{CP}$ =11 Hz, $C^{3,5}(C_6H_5)$], 106.4, 106.0 [C^4(pz)], 30.8 (m, PCH_2), 24.9 (dd, $^1J_{CP}$ = 31 Hz, $^2J_{CP}$ = 7 Hz, PCH_2) 16.6, 14.6, 13.1, 12.7 [pz*C*H$_3$].$^{31}P\{^1H\}$ NMR (161 MHz, $CDCl_3$, 25 °C, δ_P = 33.60 [s.br., $^1J_{PPt}$ = 1548 Hz, P *cis* to Br], 32.89 [s.br, $^1J_{PPt}$ = 4053 Hz, P *cis* to C≡W]. Satisfactory $^{195}Pt\{^1H\}$ NMR spectra could not be measured irrespective of solvent or temperature (–60 to +50 °C) due to poor solubility and signal multiplicity. MS (ESI, *m/z*): Found: 1135.11401. Calcd for $C_{44}H_{46}{}^{11}B^{79}BrMoN_6O_2P_2Pt$ $[M]^+$: 1135.11396. Anal. Found: C, 46.37; H, 3.95; N, 7.34%. Calcd for $C_{44}H_{46}BBrMoN_6O_2P_2Pt$: C, 46.58; H, 4.09; N, 7.41%. *Crystal data for* $C_{44}H_{46}BBrMoN_6O_2P_2Pt$, M_w = 1134.56, monoclinic, *C2/c*, *a* = 42.7794(12) Å, *b* = 10.3970(3) Å, *c* = 20.4764(7) Å, β = 94.581(3)°, *V* = 9078.3(5) Å^3, *Z* = 8, ρ_{calc} = 1.660 Mgm^{-3}, μ(Mo *K*α) = 4.35 mm^{-1}, *T* = 150(0) K, clear light yellow plate 0.27 × 0.15 ×0.07 mm, 10894 independent measured reflections (θ_{max} = 29.4 °), R_1 = 0.043, wR_2 = 0.093 for 9093 reflections [$I > 2\sigma(I)$], 545 parameters, 1 restraint. Refinement was complicated by a region of diffuse solvent which could not be adequately modelled and so a solvent mask was invoked. The algorithm determined that 116 electrons were present per solvent accessible void, which corresponds well to two molecules of chloroform (116 electrons) per unit cell. The crystal structure is presented exclusive of this solvent. See ESI (Figure S1) for molecular geometry. CDCC 1997713.

Synthesis of [WPt(μ-C)(κ^2-S_2CNEt_2)(CO)$_2$(PPh_3)(Tp*)] (7)

A solution containing [WPt(μ-C)Br(CO)$_2$(PPh_3)$_2$(Tp*)] (**1**: 156 mg, 116 μmol) and sodium *N,N*-diethyldithiocarbamate dihydrate (25 mg, 140 μmol) in toluene (20 mL) was heated under reflux for 4 hours. The resulting yellow solution was cooled and filtered through diatomaceous earth and freed of volatiles under reduced pressure producing a yellow powder. This powder was recrystallised from a mixture of CH_2Cl_2 and *n*-hexane to give a yellow microcrystalline powder that was collected by vacuum filtration, washed with *n*-hexane and dried *in vacuo* affording **7** (125 mg, 108 μmol, 93% yield). IR (CH_2Cl_2, cm^{-1}): 1935 vs ν_{CO}, 1843 vs ν_{CO}. ^1H NMR (700 MHz, $CDCl_3$, 25 °C) δ_H = 7.45 [t, $^1J_{HH}$ = 9 Hz, 3 H, C_6H_5], 7.22 [m.br, 3 H, C_6H_5], 7.02 [m.br, 6 H, C_6H_5], 5.63 [s, 1 H, pzCH], 5.59 [s, 2 H, pzCH], 3.78 [q.br, $^1J_{HH}$ = 8 Hz, 2 H, NCH_2], 3.56 [q.br, $^1J_{HH}$ = 8 Hz, 2 H, NCH_2], 2.38 [s, 15 H, $pzCH_3$], 2.26 [s, 3 H, $pzCH_3$], 1.35 [t.br., $^1J_{CP}$ = 7 Hz, 3 H, CH_2CH_3], 1.17 [t.br., $^1J_{CP}$ = 7 Hz, 3 H, CH_2CH_3]. $^{13}C\{^1H\}$ NMR (176 MHz, $CDCl_3$, 25 °C) δ_C = 338.4 [d, $^2J_{CP}$ = 6 Hz, W≡C–Pt], 227.0 [$^1J_{CW}$ = 177 Hz, CO], 208.3 [S_2C], 152.2, 151.7 [C^5(pz)], 144.1, 143.0 [C^3(pz)], 134.4 [d, $^2J_{CP}$ = 11 Hz, $C^{2,6}(C_6H_5)$], 130.5 [$C^4(C_6H_5)$], 130.3 [d, $^1J_{CP}$ = 57 Hz, $C^1(C_6H_5)$], 127.8 [d, $^3J_{CP}$ = 11 Hz, $C^{3,5}(C_6H_5)$], 106.2, 105.9 [C^4(pz)], 44.8, 43.8 [NCH_2], 16.5 15.4 12.8 12.6 [$pzCH_3$], 12.7 12.5 [CH_2CH_3]. $^{31}P\{^1H\}$ NMR (162 MHz, $CDCl_3$, 25 °C) δ_P = 13.68 [$^1J_{PPt}$ = 3880 Hz]. $^{195}Pt\{^1H\}$ NMR (85.7 MHz, $CDCl_3$, 25 °C) δ_{Pt} = –3828 [d, $^1J_{PtP}$ = 3889 Hz]. MS (ESI, *m/z*): Found: 1154.22514 Calcd for $C_{41}H_{47}BN_7NaO_2PPtS_2W$ $[M]^+$: 1154.22876. Anal. Found: C, 40.30; H, 3.35; N, 7.55%. Calcd for $C_{41}H_{47}BN_7O_2PPtS_2W.CH_2Cl_2$: C, 40.69; H, 2.98; N, 7.91%. *Crystal data for* $C_{41}H_{47}BN_7O_2PPtS_2W$, M_w = 1154.69, triclinic, $P\bar{1}$ (No. 2), *a* = 12.5263 (2) Å, *b* = 12.9390 (2) Å, *c* = 13.8769 (2) Å, α = 76.435 (1)°, β = 89.141 (1)º γ = 82.519 (1)°, *V* = 2167.50 (6) Å^3, *Z* = 2, ρ_{calc} = 1.769 Mgm^{-3}, μ(Cu *K*α) = 12.37 mm^{-1}, *T* = 150(0) K, clear

light yellow plate 0.13 × 0.05 × 0.03 mm, 8662 independent measured reflections (θ_{max} = 73.6), R_1 = 0.027, wR_2 = 0.071 for 7905 reflections [$I > 2\sigma(I)$], 513 parameters and no restraints. CDCC 1997714.

Synthesis of [WPt(μ-C)(κ³-terpy)(CO)₂(Tp*)] [PF₆] [8]PF₆

This compound was prepared via an alternative protocol to the published procedure.[2m] The present protocol provides a proof of concept but is inferior to the published method. A sample of [WPt(μ-C)Br(CO)$_2$(PPh$_3$)$_2$(Tp*)] (**1**: 100 mg, 76 μmol) and 2,2′:6′,2″-terpyridine (terpy: 14 mg, 60 μmol) was dissolved in CH_2Cl_2 (10 mL) to give an orange solution. A solution of $NaPF_6$ (14 mg, 83 μmol) in MeOH (2 mL) was added and then left to stir for 16 hours over which time the solution changed to a deep purple/orange colour. The volatiles were removed under reduced pressure to afford an orange/pink residue. This was purified by anaerobic flash column chromatography (neutral alumina, CH_2Cl_2/MeCN gradient), where neat CH_2Cl_2 eluted unreacted **1** as an orange band and neat MeCN subsequently eluted a purple band. A subsequent recrystallisation of the purple eluate by addition of toluene followed by slow removal of MeCN under reduced pressure to afford a purple solid. This was collected by vacuum filtration and washed with toluene (2 x 10 mL) and Et_2O (2 x 10 mL) before drying *in vacuo* overnight, resulting in [**8**]PF_6 (16 mg, 14 μmol, 25% isolated yield). Spectroscopic data matched those of the reported compound, however, a previously imprecisely identified (HMBC) resonance was also directly recorded. $^{13}C\{^1H\}$ NMR (151 MHz, CD_3CN, 25 °C) δ_C = 367.7 (W≡C–Pt). The complex was previously structurally characterised (CCDC 1945291).[2m]

Synthesis of [WPt(μ-C)(κ²-phen)(CO)₂(PPh₃)(Tp*)] [PF₆] [9]PF₆

Note: This compound exists as a mixture of inseparable isomers in a ratio of ~1:3. This has been attributed to the orientation of the phenanthroline ligand either distal to or occupying the cleft of the Tp* ligand. A sample of [WPt(μ-C)Br)CO$_2$(PPh$_3$)$_2$(Tp*)] (**1**: 101 mg, 75 μmol) and 1,10-phenthroline (phen: 10 mg, 55 μmol) was dissolved in CH_2Cl_2 (10 mL) to give an orange solution. A solution of $NaPF_6$ (24 mg, 84 μmol) in MeOH (2 mL) was added and the mixture was then left to stir for 16 hours during which time an orange/brown colour developed. The solvent was removed under reduced pressure to afford a brown residue which was then purified by anaerobic flash column chromatography (silica gel, gradient elution), where CH_2Cl_2 eluted excess unreacted **1** and neat THF eluted a brown band (72 mg). A subsequent crystallisation of the brown eluate from a mixture of CH_2Cl_2 and EtOH afforded a brown microcrystalline solid which was collected via vacuum filtration and washed with toluene (2 x 10mL) and Et_2O (2 x 10mL). Drying *in vacuo* for 2 hours provided the [**9**]PF_6 (56 mg, 42 μmol, 76% isolated yield).

Rotational isomers were present in a 1:5 mixture. Data reported here correspond to the major isomer however due to this unavoidable mixture, absolute assignments are occasionally equivocal. IR (CH_2Cl_2, cm^{-1}): 1968 vs υ_{CO}, 1874 vs υ_{CO}. ^1H NMR (400 MHz, $CDCl_3$, 25 °C) δ_H = 9.05 [m, 1 H, phenCH], 8.62 [t, $^1J_{HH}$ = 9 Hz, 2 H, phenCH], 8.14 [m, 3 H, phenCH], 7.95 [dd, $^1J_{HH}$ = 12, $^2J_{HH}$ = 8 Hz, 6 H, C_6H_5], 7.60 [m, 3 H, C_6H_5], 6.53 [m, 6 H, C_6H_5], 7.11 [s.br., 1 H, phenCH], 6.77 [t, $^1J_{HH}$ = 7 Hz, 1 H, phenCH], 5.81 [s, 2 H, pzCH], 5.67 [s, 1 H, pzCH], 2.67 [s, 6 H, pzCH$_3$], 2.51 [s, 6 H, pzCH$_3$], 2.46 [s, 3 H, pzCH$_3$], 2.38 [s, 3 H, pz*C*H$_3$], 2.32 [s, 3 H, pzCH$_3$], 2.09 [s, 2 H, pzCH$_3$]. $^{13}C\{^1H\}$ NMR (151 MHz, $CDCl_3$, 25 °C) δ_C = 324.7 [d, $^2J_{CP}$ = 8 Hz, W≡C–Pt], 228.7 [$^1J_{CW}$ = 174 Hz, CO], 153.7, 152.5 [$C^{6,6'}$(phen)], 152.2, 151.9 [C^5(pz)], 146.5 [C^2(phen)], 145.9[$C^{2'}$(phen)], 145.4 145.0 [C^3(pz)], 140.6, 140.5 [C^4(phen)], 135.3 [d, $^3J_{CP}$ = 12 Hz, $C^{3,5}(C_6H_5)$], 132.4 [$C^4(C_6H_5)$], 131.1 [C^5(phen)], 129.4 [d, $^2J_{CP}$ = 12 Hz, [$C^{2,6}(C_6H_5)$], 128.7 [d, $^1J_{CP}$ = 64 Hz, $C^1(C_6H_5)$], 125.4 [$C^{13,14}$(phen)], 107.3, 106.5 [C^4(pz)], 17.2, 15.0, 13.0, 12.7 [pz*C*H$_3$]. $^{19}F\{^1H\}$ NMR (376 MHz, $CDCl_3$, 25 °C) δ_F = –73.28 [d, $^1J_{FP}$ = 713 Hz, PF_6]. $^{31}P\{^1H\}$ NMR (162 MHz, $CDCl_3$, 25 °C) δ_P = 15.73 [s, $^1J_{PPt}$ = 4341 Hz, PPh_3], –144.33 [septet, $^1J_{PF}$ = 712 Hz, PF_6]. $^{195}Pt\{^1H\}$ NMR (85.7 MHz, $CDCl_3$, 25 °C) δ_P = –3619 [d, $^1J_{PtP}$ = 4428 Hz]. MS (ESI, *m/z*): Calcd for $C_{48}H_{45}BN_8O_2PPtW$ $[M]^+$: 1186.26645. Found: 1186.26721. Anal. Calcd for $C_{48}H_{45}BF_6N_8O_2P_2PtW$: C, 43.30; H, 3.41; N, 8.42 %. Found: C, C, 43.18; H, 3.31; N, 8.23 %..

Synthesis of [WPt(μ-C)(κ²-bipy)(CO)₂(PPh₃)(Tp*)] [PF₆] [10a]PF₆

A sample of [WPt(μ-C)Br(CO)$_2$(PPh$_3$)$_2$(Tp*)] (**1**: 103 mg, 76 μmol) and 2,2′-bipyridine (bipy: 34 mg, 218 μmol) was dissolved in CH_2Cl_2 (10 mL) to give an orange solution. A solution of $NaPF_6$ (24 mg, 143 μmol) in MeOH (2 mL) was added and then the mixture was stirred for 4 hours during which time the solution darkened to an orange/brown colour. The solvent was removed under reduced pressure to afford a brown residue. This was then purified by anaerobic flash column chromatography (silica gel, gradient elution CH_2Cl_2:THF), where neat THF eluted a brown band (78 mg) which was freed of volatiles. A subsequent crystallisation of the residue from concentration of a CH_2Cl_2/EtOH mixture under reduced pressure afforded [**10a**]PF_6 as a brown solid (42 mg, 42 μmol, 55% isolated yield). Crystals of a chloroform solvate suitable for X-ray diffractometry were obtained by vapour diffusion of *n*-hexane into a solution of [**10a**]PF_6 in $CHCl_3$ at 5 °C. IR (CH_2Cl_2, cm^{-1}): 1967 vs ν_{CO}, 1953 sh ν_{CO}, 1875 vs ν_{CO}, 1863 sh ν_{CO}. ^1H NMR (400 MHz, $CDCl_3$, 25 °C) δ_H = 8.87 (s.br., 1 H, bpyCH), 8.50 (d, $^1J_{HH}$ = 7 Hz, 2 H, bpyCH), 8.07 (m, 2 H, bpyCH), 7.91 (dd, $^1J_{HH}$ = 12 Hz, $^2J_{HH}$ = 8 Hz, 5 H, C_6H_5), 7.59 (m, 3 H, C_6H_5), 7.52 (m, 6 H, C_6H_5), 7.29 (d, $^1J_{HH}$ = 6 Hz, 1 H, bpyCH), 7.10 (s.br., 1 H, PPh), 6.85 (t, $^1J_{HH}$ = 7 Hz, 1 H, bpyCH), 6.36 (t, $^1J_{HH}$ = 7 Hz, 1 H, bpyCH), 5.83 (s, 2 H, pzCH), 5.64 (s, 1 H, pzCH), 2.67 (s, 6 H, pzCH$_3$), 2.46 (s, 6 H, pzCH$_3$), 2.30 (s, 3 H, pz*C*H$_3$), 2.06 (s, 3 H, pzCH$_3$) ppm. $^{13}C\{^1H\}$ NMR (151 MHz, $CDCl_3$, 25 °C) δ_C = 325.8 (d, $^2J_{CP}$ = 9 Hz, W≡C–Pt), 228.6 (CO), 155.9 155.1 [C^2(bpy)], 152.2, 151.9 [C^5(pz)], 151.1, 150.7 [C^5(bpy)] , 145.4, 144.7 [C^3(pz)], 141.5, 141.4 [C^4(bpy)], 135.2 [d, $^3J_{CP}$ = 11 Hz, $C^{3,5}(C_6H_5)$], 132.3 [$C^4(C_6H_5)$], 129.4 [d, $^2J_{CP}$ = 11 Hz, $C^{2,6}(C_6H_5)$], 128.8 [d, $^1J_{CP}$ = 64 Hz, $C^1(C_6H_5)$], 126.4, 125.3, 124.8, 124.5 [$C^{3,5}$(bpy)], 107.2, 106.5 [C^4(pz)], 17.2, 14.9, 12.9, 12.7 (pzCH$_3$). $^{19}F\{^1H\}$ NMR (377 MHz, $CDCl_3$, 25 °C) δ_F = –73.47 (d, $^1J_{FP}$ = 712 Hz) ppm. ^{31}P NMR (162 MHz, $CDCl_3$, 25 °C) δ_P = 16.37 (s, $^1J_{PPt}$ = 4293 Hz, PPh_3), –144.28 (sept., $^1J_{PF}$ = 709 Hz, PF_6). $^{195}Pt\{^1H\}$ NMR (85.7 MHz, $CDCl_3$, 25 °C) δ_{Pt} = –3587 (d, $^1J_{PtP}$ = 4265 Hz). MS (ESI, *m/z*): Calcd for $C_{46}H_{45}BN_8O_2PPtW$ $[M]^+$: 1162.26642. Found: 1162.26672. Anal. Calcd for

$C_{46}H_{45}BF_6N_8O_2P_2PtW$: C, 42.25; H, 3.47; N, 8.57 %. Found: C, 42.10; H, 3.39; N, 8.36 %. *Crystal data for* $C_{46}H_{45}BN_8O_2PPtW{\bullet}2(CHCl_3){\bullet}F_6P$, M_w = 1546.32, triclinic, $P\bar{1}$ (No. 2), a = 9.5287(2) Å, b = 16.3575(4) Å, c = 18.2918(2) Å, α = 84.892(2)°, β = 78.583(2)°, γ = 85.769(2)°, V = 2778.94(10) Å^3, Z = 2, ρ_{calc} = 1.848 Mgm^{-3}, μ(Cu $K\alpha$) = 12.18 mm^{-1}, T = 150(0) K, clear light orange plate 0.19 × 0.05 × 0.04, 10934 independent measured reflections (θ_{max} = 73.3 °), R_1 = 0.045, wR_2 = 0.125 for 9217 reflections [$I > 2\sigma(I)$], 682 parameters, no restraints. CDCC 1997715.

Synthesis of [WPt(μ-C)(κ²-dtbbpy)(CO)$_2$(PPh$_3$)(Tp*)] [PF$_6$] [10b]PF$_6$

Note: This compound exists as a mixture of inseparable isomers in a ratio of ~1:5, likely due to the orientation of bipyridyl either distal to, or occupying, the cleft of the Tp* ligand. A sample of [WPt(μ-C)Br(CO)$_2$(PPh$_3$)$_2$(Tp*)] (**1**: 102 mg, 76 μmol) and 4,4′-ditertbutyl-2,2′-bipyridine (tdbbpy: 26 mg, 97 μmol) was dissolved in CH_2Cl_2 (10 mL) to give an orange solution. A solution of $NaPF_6$ (24 mg, 143 μmol) in MeOH (2 mL) was added and the mixture then left to stir for 16 hours during which time the solution darkened to a yellow/brown colour. The solvent was removed under reduced pressure to afford a brown residue. This was then purified by anaerobic flash column chromatography (silica gel, CH_2Cl_2/THF gradient), which eluted a dark yellow band. Solvent was evaporated to give a dark yellow solid. Ultrasonic trituration in Et_2O resulted in formation of a brick red solid and yellow supernatant phase. The red solid was collected via vacuum filtration and washed with Et_2O (2 x 10 mL) before drying *in vacuo* to give [**10b**]PF_6 as a red powder (80 mg, 71 μmol, 94% isolated yield). Crystals suitable for X-ray diffractometry were grown by vapour diffusion of *n*-hexane into a solution of [**10b**]PF_6 in $CHCl_3$ at 5 °C. Rotational isomers present in a 1:5 mixture. Data reported here correspond to the major isomer however, due to this unavoidable mixture, absolute assignments were not always possible. ^{1}H NMR (400 MHz, $CDCl_3$, 25 °C): δ_H = 8.62 [dd, $^1J_{HH}$ = 6, 4 Hz, 1 H, bpyCH], 8.17 [m, 2 H, C_6H_5], 7.89 [m, 6 H, C_6H_5], 7.58 [m, 2 H, C_6H_5], 7.52 [m, 5 H, C_6H_5], 7.19 [d, $^1J_{HH}$ = 6 Hz, 1 H, bpyCH], 7.10 [m, 2 H, bpyCH], 6.81 [dd, $^1J_{HH}$ = 6, 2 Hz, 1 H bpyCH], 6.20 [d, $^1J_{HH}$ = 5 Hz, 1 H, bpyCH], 5.81 [s, 2 H, pzCH], 5.64 [s, 1 H, pzCH], 2.69 [s, 6 H, pzCH_3], 2.47 [s, 6 H, pzCH_3] 2.30 [s, 3 H, pzCH_3], 2.07 [s, 3 H, pzCH_3], 1.33, 1.30 [s x 2, 9 H x 2, C(CH_3)$_3$]. ^{13}C{^{1}H} NMR (176 MHz, $CDCl_3$, 25 °C): δ_C = 329.6 [m, W≡C–Pt], 228.7 (CO), 166.1, 165.8 [C^4(dtbbpy)], 155.8 155.0 [C^2(dtbbpy)], 152.2, 152.1 [C^5(pz)], 150.6, 150.5 [C^6(dtbbpy)], 145.4, 144.4 [C^3(pz)], 135.2 [d, $^3J_{CP}$ = 12 Hz, C^{3,5}(C_6H_5)], 132.2 [C^4(C_6H_5)], 129.3 [d, $^2J_{CP}$ = 11 Hz, C^{2,6}(C_6H_5)], 128.9 [d, $^1J_{CP}$ = 63 Hz, C^1(C_6H_5)], 123.6, 122.0, 120.9, 120.4 [C^{3,5}(dtbbpy)], 107.1, 106.4 [C^4(pz)], 36.0, 35.8 [*C*Me$_3$], 30.0 [C(*C*H$_3$)$_3$], 17.2, 15.4, 14.9, 12.8, 12.7 [pzCH_3]. ^{19}F{^{1}H} NMR (377 MHz, $CDCl_3$, 25 °C): δ_F = –73.08 [d, $^1J_{FP}$ = 713 Hz, PF_6]. ^{31}P{^{1}H} NMR (162 MHz, $CDCl_3$, 25 °C): δ_P = 16.25 [s, $^1J_{PPt}$ = 4250 Hz, PPh], –144.39 [sept., $^1J_{PF}$ = 711 Hz, PF_6]. ^{195}Pt{^{1}H} NMR (85.7 MHz, $CDCl_3$, 25 °C): δ_{Pt} = –3580 [d, $^1J_{PtP}$ = 4287 Hz]. Calcd for $C_{54}H_{61}BF_6N_8O_2P_2PtW$: C, 45.68; H, 4.33; B, 0.76; F, 8.03; N, 7.89; *Crystal data for* $C_{54}H_{61}BN_8O_2PPtW{\cdot}F_6P$, M_w = 1419.79, *triclinic*, $P\bar{1}$ (No. 2), a = 11.6701(3) Å, b = 11.7291(4) Å, c = 21.3711(7) Å, α = 79.857(3)°, β = 86.505(2)°, γ = 75.021(2)°, V = 2781.34(15) Å^3, Z = 2, ρ_{calc} = 1.695 Mgm^{-3}, μ(Mo $K\alpha$) = 4.70 mm^{-1}, T = 150(0) K, lustrous dark red block 0.31 × 0.22 × 0.13 mm, 12829 independent measured reflections (θ_{max} = 29.4°), R_1 = 0.031, wR_2 = 0.061 for 11075 reflections [$I > 2\sigma(I)$], 691 parameters, 1 restraint. CDCC 1997716.

Synthesis of [WPt(μ-C)(CO)$_2$(PPh$_3$)(κ²-Bp*)(Tp*)] (11)

Note: This compound exists as a 1:1 mixture of rotomers. A mixture of [WPt(μ-C)Br(CO)$_2$(PPh$_3$)$_2$(Tp*)] (**1**: 102 mg, 75.6 μmol) and K[Bp*] (43 mg, 178 μmol) was heated under reflux in CH_2Cl_2 (10 mL) for 16 hours. The initially orange solution evolved in colour to yellow. The solvent was removed under reduced pressure to give an orange solid. Anaerobic flash column chromatography (silica gel, 67 % CH_2Cl_2/Petroleum Ether, isocratic elution) was performed on the orange residue eluting a major orange component. Volatiles were removed prior to subjecting the residue to ultrasonic trituration in *n*-hexane (10 mL) to afford a yellow solid and a red supernatant phase. The supernatant phase was decanted and discarded and the solid was further triturated with *n*-hexane (2 x 10 mL). The yellow solid was dried *in vacuo* for 2 h to provide **11** (22 mg, 22 μmol, 29 % yield). Crystals of a chloroform solvate suitable for X-ray diffractometry were grown by vapour diffusion of *n*-hexane into a solution of **11** in $CHCl_3$.

Rotational isomers are present in a 1:1 mixture. Data collected did not indicate a predominant species, hence signals reported are for both species consistent with their relative assignments. Integrals are relative to the isomer present and hence have been normalised. It is for this reason that absolute assignments could not be assigned in some cases. IR (CH_2Cl_2, cm^{-1}): 1946 vs ν_{CO}, 1853 vs ν_{CO}. ^{1}H NMR (600 MHz, $CDCl_3$, 25 °C): δ_H = 7.48 – 7.36 [m, 4 H, C_6H_5], 7.23 – 6.98 [m, 10H, C_6H_5], 5.85, 5.79, 5.68, 5.59, 5.58, 5.53, 5.50, 5.25, 5.11, 5.02 [s x 10, 1 H x 10, pz*CH*], 2.84, 2.80, 2.72, 2.39 [s x 4, 3 H x 4, pzCH_3], 2.34 [s, 6 H pzCH_3], 2.32 [s, 3 H pzCH_3], 2.30 [overlapping s x 3, 9 H, pzCH_3], 2.27 [s, 3 H pzCH_3], 2.22 [s, 9 H pzCH_3], 2.17, 2.08, 1.96, 1.55, 1.33, 1.30 [s x 6, 3 H x 6 pzCH_3]. ^{13}C{^{1}H} NMR (151 MHz, $CDCl_3$, 25 °C): δ_C = 338.3 [d, $^2J_{CP}$ = 9 Hz, W≡C–Pt], 332.6 [d, $^2J_{CP}$ = 11 Hz, W≡C–Pt], 233.4 [$^1J_{CW}$ = 176.0 Hz, CO], 231.5 [$^1J_{CW}$ = 178 Hz, CO], 228.5 [$^1J_{CW}$ = 176 Hz, CO], 225.0 [$^1J_{CW}$ = 181 Hz, CO], 153.6, 152.5, 151.9, 151.7, 151.6, [C^5(Wpz)], 148.48, 148.45, 147.91, 147.88 [C^5(Ptpz)], 147.4, 147.2 [C^3(Ptpz)], 144.8, 144.7, 144.6, 144.0, 143.8 143.6, 143.0, 142.5 [C^3(Wpz)], 135.8–134.1 [br, C^{2,6}(C_6H_5)], 130.6 – 130.0 [m, C^{3,5}(C_6H_5)], 129.3 [d.br., $^1J_{CP}$ = 61 Hz, C^1(C_6H_5)], 128.1, 127.3 [bs, PPh], 106.6, 105.9, 105.8, 105.2, 105.0, 104.8, 104.63, 104.60 [C^4(pz)], 18.7, 17.9, 16.0 15.3, 14.9, 14.8, 14.1, 13.1, 13.0, 12.9, 12.8, 12.7, 12.64, 12.59, 12.55, 12.2 [pzCH_3]. ^{31}P{^{1}H} NMR (162 MHz, $CDCl_3$, 25 °C): δ_P = 7.52 [s, $^1J_{PPt}$ = 4285 Hz], 5.38 [s, $^1J_{PPt}$ = 4161 Hz]. ^{195}Pt{^{1}H} NMR (85.7 MHz, $CDCl_3$, 25 °C): δ_{Pt} = –3495 [d, $^1J_{PtP}$ = 4178 Hz], –3477 [d, $^1J_{PtP}$ = 4297 Hz]. MS (ESI, *m/z*): Found: 1209.3442. Calcd for $C_{46}H_{53}B_2N_{10}O_2PPtW$ [M]$^+$: 1209.3459. Anal. Found: C, 44.49; H, 4.48; N, 10.51%. Calcd for $C_{46}H_{53}B_2N_{10}O_2PPtW$: C, 44.43; H, 4.50; N, 10.50%. *Crystal data for* $C_{46}H_{53}B_2N_{10}O_2PPtW{\cdot}(CHCl_3)$, M_w = 1328.88, triclinic, $P\bar{1}$ (No. 2), a = 10.1322(6) Å, b = 14.7017(8) Å, c = 19.3416(7) Å, α = 103.794(4)°, β = 102.422(4)°, γ = 106.487(5)°, V = 2556.3(2) Å^3, Z = 2, ρ_{calc} = 1.726 Mgm^{-3}, μ(Cu $K\alpha$) = 11.27 mm^{-1}, T = 150(0) K, clear light yellow plate 0.09

× 0.05 × 0.04 mm, 9298 independent measured reflections (θ_{max}= 72.8 °), R_1 = 0.048, wR_2 = 0.127 for 6912 reflections [$I > 2\sigma(I)$], 625 parameters, 2no restraints. CDCC 1997717.

Synthesis of [WPt(μ-C)(CO)$_2$(PPh$_3$)(Tp*)$_2$] (12)

A mixture of [WPt(μ-C)Br(CO)$_2$(PPh$_3$)$_2$(Tp*)] (**1**: 152 mg, 113 μmol) and K[Tp*] (76 mg, 226 μmol) was heated under reflux in CH_2Cl_2 (10 mL) for 16 hours. The initially orange solution evolved to red during this period. The solvent was removed under reduced pressure to give an orange solid. Anaerobic flash column chromatography (silica gel, neat CH_2Cl_2, isocratic elution) was performed on the orange residue eluting a major red compound. Solvent removal was performed prior to ultrasonic trituration in *n*-hexane (10 mL) which afforded a yellow solid. The supernatant phase was decanted and the solid was dried *in vacuo* for 2 h to provide **12** (8 mg, 6 μmol, 5% yield). Crystals suitable for X-ray diffractometry were grown by vapour diffusion of *n*-hexane into a solution of **12** in $CHCl_3$.

Note: This compound exists a mixture of ~1:3 rotational isomers. It is for this reason that absolute assignments may not be appropriate on some occasions. The signals reported are for the dominant species, for which relative integrals are given. IR (CH_2Cl_2, cm^{-1}): 1947 vs ν_{CO}, 1854 vs ν_{CO}. ^{1}H NMR (400 MHz, $CDCl_3$, 25 °C): δ_H = 8.11 [dd, $^1J_{HH}$ = 12, $^2J_{HH}$ = 7 Hz, 2 H, C_6H_5], 7.90 [dd, $^1J_{HH}$ = 13, $^2J_{HH}$ = 7 Hz, 2 H, C_6H_5], 7.54 [d, $^1J_{HH}$ = 8 Hz, 2 H, C_6H_5], 7.47 – 7.30 [m, 6 H, PPh], 7.12 [t, $^1J_{HH}$ = 8 Hz, 1H, C_6H_5], 6.92 [t, $^1J_{HH}$ = 7 Hz, 2 H, C_6H_5], 5.78 [s, 2 H, pzCH], 5.60, 5.53, 5.45, 5.27 [s x 4, 1 H x 4, pzCH], 2.51, 2.39, 2.37, 2.34, 2.32, 2.24, 2.20, 2.15, 2.08, 1.72, 1.60, 1.51 [s x 12, 3 H x 12, pzCH_3]. ^{13}C{^{1}H} NMR (151 MHz, $CDCl_3$, 25 °C): δ_C = 333.5 [d, $^2J_{CP}$ = 8, $^1J_{CW}$ = 179 Hz, W≡C–Pt], 230.7, 229.5 [$^1J_{CW}$ = 179 Hz, CO], 153.7, 151.7, 151.5, 150.4, 149.2, 147.6 [C^5(pz)], 146.9, 146.5, 143.9, 143.7, 143.5, 142.7 [C^3(pz)], 136.7 [d, $^2J_{CP}$ = 12 Hz, C^{2,6}(C_6H_5)], 136.2 [d, $^2J_{CP}$ = 12 Hz, C^{2,6}(C_6H_5)], 133.9 [d, $^2J_{CP}$ = 12 Hz, C^{2,6}(C_6H_5)], 133.4 [d, $^1J_{CP}$ = 58 Hz, C^1(C_6H_5)], 131.0, 130.3, 129.3 [C^4(C_6H_5)], j 128.3, 128.2, 127.1 [d, $^3J_{CP}$ = 12 Hz, C^{3,5}(C_6H_5)], 129.5 [d, $^1J_{CP}$ = 60 Hz, C^1(C_6H_5)], 129.2 [d, $^1J_{CP}$ = 65 Hz, C^1(C_6H_5)], 106.2, 106.0, 105.7, 105.6, 105.5 [C^4(pz)], 18.8 16.2, 15.6, 14.8, 14.2, 14.1, 13.7, 13.3, 13.0, 12.6 [pzCH_3]. ^{31}P{^{1}H} NMR (162 MHz, $CDCl_3$, 25 °C): δ_P = 3.07 [s, $^1J_{PPt}$ = 4288 Hz]. ^{195}Pt{^{1}H} NMR (85.7 MHz, $CDCl_3$, 25 °C): δ_{Pt} = –3433 [d, $^1J_{PtP}$ = 4305 Hz]. MS (ESI, *m/z*): Found: 1303.4037. Calcd for $C_{51}H_{59}B_2N_{12}O_2PPtW$ [M]$^+$: 1303.4053. Anal. Found: C, 46.82; H, 4.56; N, 12.73%. Calcd for $C_{51}H_{59}B_2N_{12}O_2PPtW$: C, 46.74; H, 4.50; N, 12.70%. *Crystal data for* $C_{51}H_{59}B_2N_{12}O_2PPtW$, M_w = 1303.63, triclinic, $P\bar{1}$ (No. 2), *a* = 10.8902(2) Å, *b* = 15.0338(4) Å, *c* = 17.0497(4) Å, α = 71.254(2)°, β = 79.943(2)º, γ = 82.947(2)°, *V* = 2596.04(11) Å^3, *Z* = 2, ρ_{calc} = 1.668 Mgm^{-3}, μ(Cu *K*α) = 9.71 mm^{-1}, *T* = 150(0) K, clear light yellow block 0.18 × 0.13 × 0.06 mm, 10286 independent measured reflections (θ_{max} = 73.6 °), R_1 = 0.022, wR_2 = 0.058 for 9765 reflections [$I > 2\sigma(I)$], 649 parameters, 17 restraints. CDCC 1997718.

Synthesis of [WPt(μ-C)(CO)$_2$(PPh$_3$){κ^2-H$_2$B(mt^{Me})$_2$}(Tp*)$_2$] (13)

Upon stirring [WPt(μ-C)Br(CO)$_2$(PPh$_3$)$_2$(Tp*)] (**1**: 99 mg, 73 μmol) with Na[H$_2$B(mt^{Me})$_2$] (24 mg, 92 μmol) in CH_2Cl_2 (10 mL), the orange solution quickly faded to a yellow colour. The mixture was stirred for a further 16 hours. The solvent was removed under reduced pressure to give an orange glass (138 mg crude). Anaerobic flash column chromatography (silica gel, isocratic elution, neat CH_2Cl_2 then 8% THF/CH_2Cl_2) was performed to elute a yellow fraction. The solvent was removed followed by crystallisation of the residue by slow evaporation of a mixture of CH_2Cl_2 into *n*-hexane under reduced pressure to provide a yellow microcrystalline powder. This was collected by vacuum filtration over a glass frit, washed and with *n*-pentane (10 mL) before drying *in vacuo* for 2 hours to provide **13** (70 mg, 56 μmol, 77% yield).

Fluxional processes operate when this compound is in solution. For this reason not all signals could be completely assigned. IR (CH_2Cl_2, cm^{-1}): 1940 vs ν_{CO}, 1848 vs ν_{CO}. ^{1}H NMR (400 MHz, $CDCl_3$, 25 °C): δ_H = 7.45 – 7.32 [m, 4 H, C_6H_5], 7.28 [s, 1H overlapping $CDCl_3$, C_6H_5], 7.24 [s, 2H overlapping $CDCl_3$, PPh], 7.19 – 7.16 [m, 5 H, C_6H_5], 7.06 [s.br., 3 H, C_6H_5], 6.82 [s, 2 H, mtCH], 6.68 [s, 2 H, mtCH], 5.60 [s, 1 H, pzCH], 5.56 [s, 2 H, pzCH], 4.47 [s.v.br, 2 H, BH], 3.80 [s, 3 H, mtCH_3], 3.64 [s, 3 H, mtCH_3], 2.38 [s, 3 H, pzCH_3], 2.36 [s, 6 H, pzCH_3], 2.34 [s, 6 H, pzCH_3], 2.22 [s, 3 H, pzCH_3]. ^{13}C{^{1}H} NMR (151 MHz, $CDCl_3$, 25 °C): δ_C = 328.8 [d, $^2J_{CP}$ = 8, $^1J_{CPt}$ = 793 Hz, W≡C–Pt], 227.9 [$^1J_{CW}$ = 178 Hz, CO], 158.3, 154.3 [C^2($C_3H_2N_2$)], 152.1, 151.6 [C^5(pz)], 143.7, 142.8 [C^3(pz)], 138.0 [C_6H_5], 134.4 [d, $^2J_{CP}$ = 11 Hz, C^{2,6}(C_6H_5)], 130.9 [d, $^1J_{CP}$ = 57 Hz, C^1(C_6H_5)], 129.5 [C^4(C_6H_5)], 127.1 [d, $^3J_{CP}$ = 11 Hz, C^{3,5}(C_6H_5)], 123.8, 123.7 [C^4($C_3H_2N_2$)], 119.1 117.9 [C^5($C_3H_2N_2$))], 106.3, 105.8 [C^4(pz)], 35.7, 34.2 [mtCH_3], 16.9, 15.4, 12.8, 12.6 [pzCH_3]. ^{31}P{^{1}H} NMR (162 MHz, $CDCl_3$, 25 °C): δ_P = 14.62 [s, $^1J_{PPt}$ = 3979 Hz]. ^{195}Pt{^{1}H} NMR (85.7 MHz, $CDCl_3$, 25 °C): δ_{Pt} = –3561 [d, $^1J_{PtP}$ = 3994 Hz]. MS (ESI, *m/z*): Found: 1245.2608. Calcd for $C_{44}H_{50}B_2N_{10}O_2PPtS_2W$ [M+H]$^+$: 1245.2640. Anal. Found: C, 42.48; H, 4.19; N, 11.37%. Calcd for $C_{44}H_{49}B_2N_{10}O_2PPtS_2W$: C, 42.43; H, 3.97; N, 11.25%. *Crystal data for* $C_{44}H_{49}B_2N_{10}O_2PPtS_2W\cdot(CHCl_3)$, M_w = 1362.93, triclinic, $P\bar{1}$ (No. 2), *a* = 11.8325(10) Å, *b* = 12.6410(5) Å, *c* = 18.1325(7) Å, α = 74.259(4)°, β = 82.640(5)º, γ = 76.417(5)°, *V* = 2531.4(3) Å^3, *Z* = 2, ρ_{calc} = 1.788 Mgm^{-3}, μ(Cu *K*α) = 12.15 mm^{-1}, *T* = 150(0) K, clear light orange plate 0.20 × 0.06 × 0.03 mm, 9945 independent measured reflections (θ_{max} = 72.7 °), R_1 = 0.061, wR_2 = 0.163 for 6644 reflections [$I > 2\sigma(I)$], 624 parameters, 18 restraints. The structural model contained a minor component (2–3%) of full molecule disorder. Due to the limited contribution, only the heavy atoms (W and Pt) could be assigned. These were modelled isotropically as introducing anisotrophy destabilised the model. CDCC 1997719.

Notes and references

‡ Abbreviations. Bp* = dihydrobis(3,5-dimethylpyrazol-1-yl)borate, Tp* = hydrotris(3,5-dimethylpyrazol-1-yl)borate, Bm^{Me} = dihydrobis(*N*-methyl-2-mercaptoimidazol-1-yl)borate, bipy = 2,2'-bipyridyl, dtbbpy = 4,4'di.*tert*.butyl-2,2-bipyridyl, phen = 1,10-phenanthroline.

1 (a) D. Mansuy, J. P. Lecomte, J. C. Chottard and J. F. Bartoli, *Inorg. Chem.,* 1981, **20**, 3119-3121. (b) R. L. Miller, P. T. Wolczanski and A. L. Rheingold, *J. Am. Chem. Soc.,* 1993, **115**, 10422-10423. (c) E. Solari, S. Antonijevic, S. Gauthier, R. Scopelliti and K. Severin, *Eur. J. Inorg. Chem.,* 2007, 367-371. (d) R. D. Young, A. F. Hill, G. E. Cavigliasso and R. Stranger, *Angew. Chem., Int. Ed.,* 2013, **52**, 3699-3702. (e) G. Rossi, V.

L. Goedken and C. Ercolani, *Chem. Commun.,* 1988, 46-47. (f) S. I. Kalläne, T. Braun, M. Teltewskoi, B. Braun, R. Herrmann and R. Laubenstein, *Chem. Commun.,* 2015, **51**, 14613-14616. (g) T. Ahrens, B. Schmiedecke, T. Braun, R. Herrmann and R. Laubenstein, *Eur. J. Inorg. Chem.*, 2017, 713-722. (h) Galich, A. Kienast, H. Huckstadt and H. Homborg, *Z. Anorg. Allg. Chem.,* 1998, **624**, 1235-1242. (i) C. Colomban, E. V. Kudrik, D. V. Tyurin, F. Albrieux, S. E. Nefedov, P. Afanasiev and A. B. Sorokin, *Dalton Trans.*, 2015, **44**, 2240-2251. (j) W. Beck, W. Knauer and C. Robl, *Angew. Chem., Int. Ed.*, 1990, **29**, 318-320. (k) H. J. Barnett, L. K. Burt and A. F. Hill, *Dalton Trans.,* 2018, **47**, 9570-9574. (l) A. F. Hill and L. J. Watson, *Chem. Commun.*, 2020, **56**, 2356-2359. (m) H. J. Barnett and A. F. Hill, submitted to *Chem. Commun*.

2 (a) S. L. Latesky and J. P. Selegue, *J. Am. Chem. Soc.*, 1987, **109**, 4731-4733. (b) M. Etienne, P. S. White and J. L. Templeton, *J. Am. Chem. Soc.*, 1991, **113**, 2324-2325. (c) S. H. Hong, M. W. Day and R. H. Grubbs, *J. Am. Chem. Soc.,* 2004, **126**, 7414-7415. (d) A. F. Hill, M. Sharma and A. C. Willis, *Organometallics*, 2012, **31**, 2538-2542. (e) R. L. Cordiner, A. F. Hill and J. Wagler, *Organometallics*, 2008, **27**, 5177-5179. (f) I. A. Cade, A. F. Hill and C. M. A. McQueen, *Organometallics*, 2009, **28**, 6639-6641. (g) E. S. Borren, A. F. Hill, R. Shang, M. Sharma and A. C. Willis, *J. Am. Chem. Soc.*, 2013, **135**, 4942-4945. (h) A. Reinholdt, J. Bendix, A. F. Hill and R. A. Manzano, *Dalton Trans.*, 2018, **47**, 14893-14896. (i) A. Reinholdt, A. F. Hill and J. Bendix, *Chem. Commun.,* 2018, **54**, 5708-5711. (j) W. Knauer, W. Beck *Z. Anorg. Allg. Chem.,* 2008, **634**, 2241-2245. (k) L. K. Burt, R. L. Cordiner, A. F. Hill, R. A. Manzano and J. Wagler, *Chem. Commun.,* 2020, **56**, DOI: 10.1039/D0CC02070B. (l) B. J. Frogley and A. F. Hill, *Chem. Commun.*, 2019, **55**, 12400-12403. (m) B. J. Frogley, A. F. Hill and L. J. Watson, *Chem. Eur. J.*, 2020, **26**, DOI: 10.1002/chem.202001588.

3 (a) A. Hejl, T. M. Trnka, M. W. Day and R. H. Grubbs, *Chem. Commun.,* 2002, 2524-2525. (b) A. Reinholdt, K. Herbst and J. Bendix, *Chem. Commun.,* 2016, **52**, 2015-2018. (b) A. Reinholdt, J. E. Vibenholt, T. J. Morsing, M. Schau-Magnussen, N. E. A. Reeler and J. Bendix, *Chem. Sci.,* 2015, **6**, 5815-5823. (c) A. Reinholdt and J. Bendix, *Inorg. Chem.,* 2017, **56**, 12492-12497. (d) A. Reinholdt, A. F. Hill and J. Bendix, *Chem. Commun.,* 2018, **54**, 5708-5711; (e) A. Reinholdt, S. H. Majer, R. M. Gelardi, S. N. MacMillan, A. F. Hill, O. F. Wendt, K. M. Lancaster and J. Bendix, *Inorg. Chem.,* 2019, **58**, 4812-4819.

4 (a) H. J. Barnett and A. F. Hill, *Angew. Chem., Int. Ed.*, 2020, 59, 4274-4277: Further unstable examples have been generated and spectroscopically observed at low temperatures: (b) S. Takemoto, J. Ohata, K. Umetani, M. Yamaguchi and H. Matsuzaka, *J. Am. Chem. Soc.,* 2014, **136**, 15889-15892. (c) S. Takemoto, H. Ishii, M. Yamaguchi, A. Teramoto, M. Tsujita, D. Ozeki and H. Matsuzaka, *Organometallics,* 2019, **38**, 4298-4306. (d) S. Takemoto, M. Tsujita and H. Matsuzaka, *Organometallics,* 2017, **36**, 3686-3691.

5 T. Desmond, F. J. Lalor, G. Ferguson and M. Parvez, *J. Chem. Soc., Chem. Commun.*, 1984, 75-77

6 J. Zhu, Z. Lin and T. B. Marder, *Inorg. Chem.*, 2005, **44**, 9384-9390.

7 R. Hoffmann, *Angew. Chem., Int. Ed. Engl.,* 1982, **21**, 9711-724.

8 F. G. A. Stone, *Angew. Chem., Int. Ed. Engl.,* 1984, **23**, 89-99.

9 L. J. Manojlovic-Muir and K. W. Muir, *Inorg. Chim Acta*, 1974, **10**, 47-49.

10 J. M. A. Wouters, K. Vrieze, C. J. Elsevier, M. C. Zoutberg and K. Goubitz, *Organometallics*, 1994, **13**, 1510-1513.

11 C. A. Tolman , *Chem. Rev*., 1977, **77**, 313-348.

12 L. M. Caldwell, *Adv. Organomet. Chem.*, 2008, **56**, 1-94.

13 (a) F. A. Cotton and C. S. Kraihanzel, *J. Am. Chem. Soc.,* 1962, **84**, 4432-4438; (b) C. S. Kraihanzel and F. A. Cotton, *Inorg. Chem.,* 1963, **2**, 533-540. (c) J. A. Timney, *Inorg. Chem.,* 1979, **18**, 2502-2506

14 C. Hansch, A. Leo and R. W. Taft, *Chem. Rev.*, 1991, **91**, 165-195.

15 F. J. Lalor, T. J. Desmond, G. M. Cotter, C. A. Shanahan, G. Ferguson, M. Parvez, B. Ruhl, *J. Chem. Soc., Dalton Trans.,* **1995**, 1709-1726.

16 G. M. Jamison, P. S. White, J. L. Templeton, *Organometallics* **1991**, *10*, 1954-1959.

17 Bruce, A. E.; Gamble, A. S.; Tonker, T. L.; Templeton, J. L. *Organometallics* **1987**, *6*, 1350-1352

18 R. L. Cordiner, A. F. Hill and J. Wagler, Organometallics, 2008, 27, 4532-4540.

19 A. L. Colebatch, A. F. Hill, R. Shang and A. C. Willis, *Organometallics*, 2010, **29**, 6482-6487.

20 A. L. Colebatch and A. F. Hill, *Dalton Trans.* 2017, **46**, 4355 – 4365; (b) R. L. Cordiner, P. A. Gugger, A. F. Hill and A. C. Willis, *Organometallics*, 2009, **28**, 6632-6635. (c) A. L. Colebatch, A. F. Hill and M. Sharma, *Organometallics*, 2015, **34**, 2165-2182.

21 A. E. Enriquez, P. S. White, J. L. Templeton, *J. Am. Chem. Soc.,* 2001, **123**, 4992-5002.

22 B. J. Frogley and A. F. Hill, *Chem. Commun*., 2018, **54**, 2126-2129.

23 (a) A. F. Hill and R. A. Manzano, *Dalton Trans*., 2019, 48, 6596-6610. (b) R. A. Manzano and A. F. Hill, *Adv. Organomet. Chem.*, 2019, **72**, 103-171.

24 B. J. Frogley and A. F. Hill, *Chem. Commun.*, 2019, **55**, 15077-15080.

25 B. J. Frogley, A. F. Hill, R. A. Manzano, M. Sharma, *Chem. Commun*., 2018, **54**, 1702-1705.

26 K. C. Stone, G. M. Jamison, P. S. White and J. L. Templeton, *Inorg. Chim. Acta*, 2002, **330**, 161-172.

27 D. S. Frohnapfel, P. S. White and J. L. Templeton, *Organometallics*, 2000, **19**, 1497-1506.

28 B. E. Woodworth, D. S. Frohnapfel, P. S. White and J. L. Templeton*, Organometallics,* 1998, **17**, 1655-1662.

29 B. E. Woodworth, P. S. White, J. L. Templeton, *J. Am. Chem. Soc.,* 1997, **119**, 828-829.

30 K. C. Stone, P. S. White, J. L. Templeton, *J. Organomet. Chem.,* 2003, **684**, 13-19.

31 (a) A. C. Filippou, C. Wagner, E. O. Fischer and C. Völkl, *J. Organomet. Chem.*, 1992, **438**, C15-C22. (b) A. C. Filippou, P. Hofmann, P. Kiprof, H. R. Schmidt and C. Wagner, *J. Organomet. Chem.,* 1993, **459**, 233-247.

32 G. Hogarth, *Prog. Inorg. Chem.*, 2005, **53**, 7-561.

33 (a) G. J. Irvine, C. E. F. Rickard, W. R. Roper and L. J. Wright, *J. Organomet. Chem.*, 1990, **387**, C9-12. (b) M. F. Asaro, A. Mayr, B. Kahr and D. Van Engen, *Inorg. Chim. Acta*, 1994, **220**, 335-346. (c) K. J. Harlow, A. F. Hill, T. Welton, A. J. P. White and D. J. Williams, *Organometallics*, 1998, **17**, 1916-1918. (d) D. J. Cook, K. J. Harlow, A. F. Hill, T. Welton, A. J. P. White and D. J. Williams, *New J. Chem.*, 1998, **22**, 311-314

34 (a) A. Mayr, G. A. McDermott, A. M. Dorries, A. K. Holder, W. C. Fultz and A. L. Rheingold, *J. Am. Chem. Soc.*, 1986, **108**, 310-311. (b) S. Anderson and A. F. Hill, *J. Chem. Soc., Dalton Trans.*, 1993, 587-590.

35 (a) B. Buriez, D. J. Cook, K. J. Harlow, A. F. Hill, T. Welton, A. J. P. White, D. J. Williams and J. D. E. T. Wilton-Ely, *J. Organomet. Chem.*, 1999, **578**, 264-267. (b) B. Buriez, I. D. Burns, A. F. Hill, A. J. P. White, D. J. Williams and J. D. E. T. Wilton-Ely, *Organometallics*, 1999, **18**, 1504-1516.

36 E. Román, D. Catheline, D. Astruc, P. Batail, L. Ouahab and F. Varret, *J. Chem. Soc. Chem. Comm.,* 1982, 129-131.

37 S. J. Nieter Burgmayer and J. L. Templeton, *Inorg. Chem.*, 1985, **24**, 3939-3946.

38 (a) A. L. Rheingold and D. Garza, Cambridge Crystallographic Data Centre, private Communication, 2015, CCDC 1436771. (b) D. L. Reger, Y. Ding, D. G. Garza and L. Lebioda, *J. Organomet. Chem.,* 1993, **452**, 263-270.

39 This useful reagent may alternatively and more conveniently be generated *in situ via* lithium-halogen exchange between ^{n}BuLi and [W(≡CBr)(CO)$_2$(Tp*)].[2e]

40 For more systematic synthetic approaches to *N*-heterocycle functionalized carbynes see ref 2m and B. J. Frogley and A. F. Hill, *Dalton Trans.*, 2020, **49**, 3272-3283.

41 (a) S. Trofimenko, *J. Am. Chem. Soc.* 1967, **89**, 6288-6294; (b) S. Trofimenko, *"Scorpionates: The Coordination Chemistry of Polypyrazolylborate Ligands*" Imperial College Press: London 1999; (c) C. Pettinari, "Scorpionates II: Chelating Borate Ligands" " Imperial College Press: London 2008.

42 I. R. Crossley, *Adv. Organomet. Chem.*, 2010, **58**, 109-208

43 M. D. Curtis, K. B. Shiu and W. M. Butler, *Organometallics,* 1983, **2**, 1475-1477.

44 (a) A. J. Canty, J. Patel, M. Pfeffer, B. W. Skelton and A. H. White, *Inorg. Chim. Acta*, 2002, **327**, 20-25. (b) A. J. Canty, H. Jin, B. W. Skelton and A. H. White, *Aus. J. Chem.*, 1999, **52**, 417-419. (c) A. J. Canty and H. Jin, *J. Organomet. Chem.*, 1998, **565**, 135-140. (d) A. J. Canty, S. D. Fritsche, H. Jin, J. Patel, B. W. Skelton and A. H. White, *Organometallics*, 1997, **16**, 2175-2182. (e) A. J. Canty, A. Dedieu, H. Jin, A. Milet and M. K. Richmond, *Organometallics*, 1996, **15**, 2845-2847. (f) A. J. Canty, S. D. Fritsche, H. Jin, B. W. Skelton and A. H. White, *J. Organomet. Chem.*, 1995, **490**, C18-C19. (g) P. K. Byers, A. J. Canty and R. T. Honeyman, *Adv. Organomet. Chem.*, 1992, **34**, 1-65.

45 (a) K. D. Lavoie, B. E. Frauhiger, P. S. White and J. L. Templeton, *J. Organomet. Chem.*, 2015, **793**, 182-191. (b) B. E. Frauhiger, M. T. Ondisco, P. S. White and J. L. Templeton, *J. Am. Chem. Soc.*, 2012, **134**, 8902-8910. (c) B. E. Frauhiger and J. L. Templeton, *Organometallics*, 2012, **31**, 2770-2784. (d) B. E. Frauhiger, P. S. White and J. L. Templeton, *Organometallics*, 2012, **31**, 225-237. (e) K. L. Engelman, P. S. White and J. L. Templeton, *Organometallics*, 2010, **29**, 4943-4949. (f) K. L. Engelman, P. S. White and J. L. Templeton, *Inorg. Chim. Acta*, 2009, **362**, 4461-4467. (g) M. G. MacDonald, C. N. Kostelansky, P. S. White and J. L. Templeton, *Organometallics*, 2006, **25**, 4560-4570.

46 (a) C. A. Kosky, P. Ganis and G. Avitabile, *Acta Crystallogr., Sect. B: Struct. Crystallogr. Cryst. Chem.* 1971, **B27**, 1859-1864. (b) F. A. Cotton, M. Jeremic and A. Shaver, *Inorg. Chim. Acta,* 1972, **6**, 543-551. (c) R. J. Abernethy, M. R. St.-J. Foreman, A. F. Hill, M. K. Smith and A. C. Willis, *Dalton Trans.*, 2020, **49**, 781-796.

47 (a) S. Pal, M. W. Drover, B. O. Patrick and J. A. Love, *Eur. J. Inorg. Chem.*, 2016, 2403-2408. (b) I. R. Crossley, A. F. Hill and A. C. Willis, *Organometallics*, 2005, **24**, 4889-4892.

48 (a) M. D. Spicer and J. Reglinski, *Eur. J. Inorg. Chem.*, 2009, 1553-1574. (b) M. Garner, J. Reglinski, I. Cassidy, M. D. Spicer and A. R. Kennedy, *Chem. Commun*., 1996, 1975-1976.

49 (a) B. M. Bridgewater, T. Fillebeen, R. A. Friesner and G. Parkin, *Dalton Trans.*, 2000, 4494-4496. (b) C. Kimblin, B. M. Bridgewater, D. G. Churchill, T. Hascall and G. Parkin, *Inorg. Chem.*, 2000, **39**, 4240-4243. (c) B. M. Bridgewater and G. Parkin, *J. Am. Chem. Soc.*, 2000, **122**, 7140-7141. (d) C. Kimblin, B. M. Bridgewater, T. Hascall and G. Parkin, *Dalton Trans.*, 2000, 1267-1274. (e) C. Kimblin, B. M. Bridgewater, T. Hascall and G. Parkin, *Dalton Trans.*, 2000, 891-897. (f) C. Kimblin, B. M. Bridgewater, D. G. Churchill and G. Parkin, *Chem. Commun.*, 1999, 2301-2302

50 (a) R. Garcia, A. Paulo, A. Domingos, I. Santos, K. Ortner and R. Alberto, *J. Am. Chem. Soc.,* 2000, **122**, 11240-11241. (b) I. R. Crossley, A. F. Hill, E. R. Humphrey and M. K. Smith, *Organometallics*, 2006, **25**, 2242-2247. (d) R. J. Abernethy, M. R. St.-J. Foreman, A. F. Hill, N. Tshabang, A. C. Willis and R. D.Young, *Organometallics,* 2008, **27**, 4455-4463. (e) R. J. Abernethy, A. F. Hill, N. Tshabang, A. C. Willis and R. D. Young, *Organometallics*, 2009, **28**, 488-492. (f) M. R. St-.J. Foreman, C. Ma, A. F. Hill, N. E. Otten, M. Sharma, N. Tshabang and J. S. Ward, *Dalton Trans*., 2017, **46**, 14957-14972.

51 (a) M. R. St.-J. Foreman, A. F. Hill, A. J. P. White and D. J. Williams, *Organometallics*, 2003, 22, 3831-3840. (b) P. J. Bailey, A. Dawson, C. McCormack, S. A. Moggach, I. D. Oswald, S. Parsons, D. W. H. Rankin and A. Turner, *Inorg. Chem.*, 2005, **44**, 8884-8898.

52 (a) A. F. Hill, G. R. Owen, A. J. P. White and D. J. Williams, *Angew. Chem., Int. Ed*., 1999, **38**, 2759-2761. (b) I. R. Crossley, M. R. St.-J. Foreman, A. F. Hill, G. R. Owen, A. J. P. White, D. J. Williams and A. C. Willis, *Organometallics*, 2008, **27**, 381-386. (c) M. R. St.-J. Foreman, A. F. Hill, G. R. Owen, A. J. P. White and D. J. Williams, *Organometallics*, 2003, **22**, 4446-4450. (d) M. R. St.-J. Foreman, A. F. Hill, A. J. P. White and D. J. Williams, *Organometallics*, 2004, **23**, 913-916. (e) I. R. Crossley, A. F. Hill and A. C. Willis, *Organometallics*, 2010, **29**, 326-336. (f) M. R. St.-J. Foreman, A. F. Hill, C. Ma, N. Tshabang and A. J. P. White, *Dalton Trans.*, 2019, **48**, 209-219. (g) C. Ma and A. F. Hill, *Dalton Trans*., 2019, **48**, 1976-1992.

53 For reviews on M→B polar-covalent (dative) bonding see (a) H. Braunschweig and R. D. Dewhurst, *Dalton Trans.*, 2011, **40**, 549-558. (b) A. Amgoune and D. Bourissou, *Chem. Commun.*, 2011, **47**, 859-871. (c) G. Bouhadir and D. Bourissou, *Chem. Soc. Rev.,* 2016, **45**, 1065-1079. (d) G. R. Owen, *Chem. Soc. Rev.,* 2012, **41**, 3535-3546.

54 (a) I. R. Crossley and A. F. Hill, *Organometallics*, 2004, **23**, 5656-5658. (b) I. R. Crossley and A. F. Hill, *Dalton Trans.*, 2003, 201-203 (c) I. R. Crossley, A. F. Hill and A. C. Willis, *Organometallics*, 2008, **27**, 312-315. (d) S. Bontemps, M. Sircoglou, G. Bouhadir, H. Puschmann, J. A. K.Howard, P. W. Dyer, K. Miqueu and D. Bourissou, *Chem.-Eur. J.*, 2008, **14**, 731-740. (e) S. Bontemps, G. Bouhadir, W. Gu, M. Mercy, C.-H. Chen, B. M. Foxman, L. Maron, O. V. Ozerov and D. Bourissou, *Angew. Chem., Int. Ed.,* 2008, **47**, 1481-1484. (f) G. R. Owen, P. H. Gould, A. Hamilton and N. Tsoureas, *Dalton Trans.*, 2010, **39**, 49-52. (g) A. Iannetelli, G. Tizzard, S. J. Coles, G. R. Owen, *Organometallics*, 2018, **37**, 2177-2187. (h) A. Zech, M. F. Haddow, H. Othman, G. R. Owen, *Organometallics*, 2012, **31**, 6753-6760. (i) A. Neshat, H. R. Shahsavari, P. Mastrorilli, S. Todisco, M. G. Haghighi and B. Notash, *Inorg. Chem.,* 2018, **57**, 1398-1407. (j) S. Holler, M. Tuchler, B. G. Steller, F. Belaj, L. F. Veiros, K. Kirchner and N. C. Mosch-Zanetti, *Inorg. Chem.*, 2018, **57**, 6921-6931.

55 M. R. St.-J. Foreman, A. F. Hill, N. Tshabang, A. J. P. White and D. J. Williams, *Organometallics,* 2003, **22**, 5593-5596.

56 (a) C. P. Gordon, C. Raynaud, R. A. Andersen, C. Copéret and O. Eisenstein, *Acc. Chem. Res.*, 2019, **52**, 2278-2289. (b) K. Yamamoto, C. P. Gordon, W.-C. Liao, C. Copéret, C. Raynaud and O. Eisenstein, *Angew. Chem., Int. Edit.*, 2017, **56**, 10127-10131.

57 B. M. Still, P. G. A. Kumar, J. R. Aldrich-Wright and W. S. Price, *Chem. Soc. Rev.*, 2007, **36**, 665–686.

58 A. Streitweiser and D. M. E. Reuben, *J. Am. Chem. Soc.* **1971**, **93**, 1793-1794.

59 *CrysAlisPRO,* Oxford Diffraction, Agilent Technologies UK Ltd, Yarnton, England.

60 (a) G. Sheldrick, *Acta Crystallogr. Sect. A: Found. Crystallogr.*, 2008, **64**, 112-122. (b) G. M. Sheldrick, *Acta Crystallogr. Sect. C: Cryst. Struct. Commun.*, 2015, **71**, 3-8.

61 (a) C. F. Macrae, P. R. Edgington, P. McCabe, E. Pidcock, G. P. Shields, R. Taylor, M. Towler and J. van de Streek, *J. Appl. Crystallogr.*, 2006, **39**, 453-457. (b) C. F. Macrae, I. J. Bruno, J. A. Chisholm, P. R. Edgington, P. McCabe, E. Pidcock, L. Rodriguez-Monge, R. Taylor, J. van de Streek and P. A. Wood, *J. Appl. Crystallogr.*, 2008, **41**, 466-470.

62 *Spartan18®* (2018) Wavefunction, Inc., 18401 Von Karman Ave., Suite 370 Irvine, CA 92612 U.S.A

63 (a) A. D. Becke, *J. Chem. Phys.*, 1993, **98**, 5648– 5652. (b) P. J. Stephens, F. J. Devlin, C. F. Chabalowski and M. J. Frisch*, J. Phys. Chem.*, 1994, **98**, 11623-11627.

64 (a) J.-D. Chai and M. Head-Gordon, *J. Chem. Phys.*, 2008, **128**, 0841061-18410615. (b) J.-D. Chai and M. Head-Gordon, *Phys. Chem. Chem. Phys.*, 2008, **10**, 6615-6620.
65 (a) P. J. Hay and W.R. Wadt, *J. Chem. Phys.*, 1985, **82**, 270-283. (b) W. R. Wadt and P. J. Hay, *J. Chem. Phys.*, 1985, **82**, 284-298. (c) P. J. Hay, W. R. Wadt, *J. Chem. Phys.*, 1985, **82**, 299-310.
66 W. J. Hehre, R. Ditchfeld and J. A. Pople, *J. Chem. Phys.*, 1972, **56**, 2257-2261.
67 H. J. Reich, **AX** and **AB** Spectra, https://www.chem.wisc.edu/areas/reich/nmr/05-hmr-10-ax-ab.htm, (as at 4/3/2020).